(2)

AMMRC TR-85-18

AD

RELIABILITY AND LIFE PREDICTION METHODOLOGY - M60 TORSION BARS

AD-A159 197

R. S. BARSOUM, W. M. BETHONY, R. H. BROCKELMAN, H. P. HATCH, C. F. HICKEY, Jr., W. T. MATTHEWS, and D. M. NEAL

June 1985

Approved for public release; distribution unlimited.

ARMY MATERIALS AND MECHANICS RESEARCH CENTER
Watertown, Massachusetts 02172-0001

UNCLASSIFIED

SECURITY CLASSIFICATION OF THIS PAGE (When Data Entered)

REPORT DOCUMENTATION PAGE	READ INSTRUCTIONS BEFORE COMPLETING FORM
1. REPORT NUMBER AMMRC TR 85-18 — 2. GOVT ACCESSION NO. AD-A159 197	3. RECIPIENT'S CATALOG NUMBER
4. TITLE (and Subtitle) RELIABILITY AND LIFE PREDICTION METHODOLOGY - M60 TORSION BARS	5. TYPE OF REPORT & PERIOD COVERED Final Report
	6. PERFORMING ORG. REPORT NUMBER
7. AUTHOR(s) Roshdy S. Barsoum, Wayne M. Bethony, Robert H. Brockelman, Harold P. Hatch, Charles F. Hickey, Jr., and Donald M. Neal	8. CONTRACT OR GRANT NUMBER(s)
9. PERFORMING ORGANIZATION NAME AND ADDRESS Army Materials and Mechanics Research Center Watertown, Massachusetts 02172-0001 AMXMR-SMM	10. PROGRAM ELEMENT, PROJECT, TASK AREA & WORK UNIT NUMBERS D/A Project: 1L161102AH42 Agency Accession: DA OG9431
11. CONTROLLING OFFICE NAME AND ADDRESS U.S. Army Materiel Command (AMC), Alexandria, VA 22333	12. REPORT DATE June
	13. NUMBER OF PAGES 57
14. MONITORING AGENCY NAME & ADDRESS (if different from Controlling Office)	15. SECURITY CLASS. (of this report) Unclassified
	15a. DECLASSIFICATION/DOWNGRADING SCHEDULE

16. DISTRIBUTION STATEMENT (of this Report)

Approved for public release; distribution unlimited.

Accession For	
NTIS GRA&I	X
DTIC TAB	
Unannounced	
Justification	
By	
Distribution/	
Availability Codes	
Dist	Avail and/or Special
A-1	

DTIC COPY INSPECTED

17. DISTRIBUTION STATEMENT (of the abstract entered in Block 20, if different from Report)

18. SUPPLEMENTARY NOTES

A summary of the report was presented at the Army Solid Mechanics Conference in Rhode Island, October 1, 1984.

19. KEY WORDS (Continue on reverse side if necessary and identify by block number)

Reliability,	Torsion bars,	Nondestructive testing,
Life expectancy,	Probability,	Random vibration,
Failure,	Mechanical properties,	Maintenance.
	Fracture (mechanics),	

20. ABSTRACT (Continue on reverse side if necessary and identify by block number)

(SEE REVERSE SIDE)

DD FORM 1 JAN 73 1473 EDITION OF 1 NOV 65 IS OBSOLETE

UNCLASSIFIED

SECURITY CLASSIFICATION OF THIS PAGE (When Data Entered)

UNCLASSIFIED

SECURITY CLASSIFICATION OF THIS PAGE (When Data Entered)

Block No. 20

ABSTRACT

The life prediction and reliability assessment of the M60 tank torsion bars were obtained from applying a methodology involving several disciplines. The disciplines included: structural mechanics, fracture mechanics, statistical reliability, mechanical testing, nondestructive examination (NDE), quality assurance (QA), and metallurgical and fractographic evaluations.

The methodology was applied in order to obtain a procedure for increasing torsion bar life and enhance the reliability of the M60 tank. U.S. Army reliability performance is commonly measured in mean miles between failures (MMBF). In order to introduce a more meaningful measure of component acceptability, this report describes methods for obtaining minimum life estimate at a specified probability of survival using the Monte Carlo process. This includes predicting remaining life with known risk and an approach to perform trade-off costs or redesign for increased life. The result is a more meaningful measure of component acceptability. The reliability versus bar life computation indicated a negligible amount of life after a bar flaw was initiated in the bar. The minimum life estimates prior to crack initiation were in good agreement with frequency of actual bar failures recorded at Aberdeen Proving Grounds. Originator supplied

keywords include:

Fiche 19

UNCLASSIFIED

SECURITY CLASSIFICATION OF THIS PAGE (When Data Entered)

CONTENTS

I. INTRODUCTION

The M60 tank (Figure 1), which was developed in the 1960's, is still the principal Army heavy tank. It is currently undergoing a major "Rebuild" program to increase its effectiveness. The M60 program manager has expressed concern regarding the reliability of various components of the overhauled tanks as a result of failures experienced during proving ground tests. In a report to Congress, January 29, 1980, the GAO expressed a similar concern on the reliability of other systems. This study is an effort by an interdisciplinary task group assembled at AMMRC from specialists in material science, engineering, structural mechanics, nondestructive testing, and statistical analysis. The charter of the task group was to develop a methodology for life prediction of structural components in the M60 tank. The torsion bar (Figures 2 and 3) was chosen because of the availability of a data base obtained from a comprehensive research at AMMRC, proving grounds and overhaul depots. It should be noted that the torsion bar performs like a spring by providing the necessary motion for the wheel to follow the terrain. The M60 has six torsion bars on each side. The front and rear wheel arms have shock absorbers and stops, while the intermediate wheel arms have only stops to limit their motion. Torsion bar failure can lead to reduced mobility and track throwing, or failure to other overloaded bars and eventual total loss of mobility of the tank.

The task groups made visits to manufacturing facilities, the overhaul depot, field test sites, AMSAA, and TACOM in order to obtain data and background information. Detailed failure analysis metallurgical examination, material testing, NDE, detailed stress analysis, and a comprehensive probablistic analysis were completed by the group. The paper will discuss in detail the above studies, including major findings of a sensitivity analysis, and the final conclusions with regards to design improvements, material requirements, and the feasibility of predictive methodology for torsion bars. The methodology used here circumvents the present deterministic approaches used in establishing design life. It simulates variability of loading and material by introducing Monte Carlo methods.[1]

II. RELIABILITY AND LIFE PREDICTION METHODOLOGY

The approach taken to developing life prediction methodology was basically to obtain as much data about the torsion bar as the program would allow, analyze the data, perform the reliability study, and make recommendations.

The M60 task group visited various manufacturers of the torsion bars and obtained quality assurance procedures, test results, manufacturing procedures, and machining methods (General Dynamics and FMC). The developer, the Army Tank-Automotive Command (TACOM), provided the task group with the requirements and specifications, Depot Maintenance Work Requirement (DMWR),[2] described the user experiences. Aberdeen Proving Ground (APG) test facilities and the Materials Testing Directorate provided spectrum load data from a specific course. They also carefully monitored bar failures. The Anniston Army overhaul depot described inspection procedures information, NDE, and replacement requirements. A major part of the material data generated, involved mechanical and various metallurgical properties, and their relation to the specification. These properties were then incorporated with the data bank obtained from the QA testing of the manufacturer and published data on the material.

1. NEAL, D. M., and MASON, D. S. *Determination of Structural Reliability Using a Flaw Simulation Scheme.* Army Materials and Mechanics Research Center, AMMRC TR 81-53, October 1981.
2. *Suspension System Components for M60.* Depot Maintenance Work Requirement, TACOM, DMWR9-2350-253-1-5.

The methodology then required accurate analysis of the mechanical loading, stresses, fatigue, and fracture evaluation of the torsion bar.

Finally, all the data is incorporated in a Monte Carlo method in order to determine the reliability of the torsion bar. This method requires modeling of the spectrum loads and the material fatigue life with respect to crack growth or stress/cycles to failure (S/N). The reliability of a single torsion bar (or system) can then be studied under various assumptions of terrain, speed, improvement in designer material, inspection procedure, replacement period or any combinations.

III. MATERIAL CHARACTERIZATION DATA

Several sources were used in obtaining material properties. These covered QA data obtained from the manufacturer, mechanical and metallurgical tests performed at AMMRC by the task group, published material data, and discussions with the other torsion bars manufacturers.

The M60 torsion bars are currently being manufactured by General Dynamics (GD, Scranton, PA) and Machine Products Co., according to MIL-5-45387A, from AISI 8660 steel. It should be noted that the bar specifications do not have an explicit requirement for fracture toughness or Charpy impact energy and the only requirement is placed on Rockwell Hardness. The metallurgical data reported here was obtained from the failed torsion bars obtained from Aberdeen Proving Grounds (APG) and Anniston Army Depot.

Fatigue Data

As part of the quality assurance (QA) requirements, several torsions bars from each heat were tested. The torsional test machine is similar to that shown in Figure 4. The QA data obtained from GD, shown in Table 1, was that of the number of cycles to failure of the torsion bar for a specified prescribed angle of twist (42°) which is based on the maximum allowable torsional shear stress of 140 ksi. Table 1 also shows the cause and location of failure in each test. This data is represented by the probability of failure versus number of cycles to failure (Figures 5 through 8) for the individual years 1978-1982. The Kruskal-Wallis multi-sample test for identical populations,[3] showed that there are no significant differences among individual yearly fatigue test results, therefore, the data was pooled together. The data shown in Figure 9 is the accumulation from test results on the various heats of production from 1977-1982. The 1983 data were not included as they represent a new bar modification.

The QA specification requires that three bars be tested for every heat with at least 45,000 fatigue cycles obtained prior to bar failure. The approach currently used by the manufacturers is to run the test until the torsion bar fails (Table 1). In many instances the fatigue test machine has failed, due to the excessively large number cycles required resulting in an increased cost for quality control. In order to overcome this difficulty a statistical procedure was applied using a Weibull censored data analysis[4] approach. This procedure obtains the design allowable

3. HOLLANDER, M., and WOLFE, D. A. *Nonparametric Statistical Methods.* John Wiley & Sons, New York, 1973.
4. LAWLESS, J. F. *Contruction of Tolerance Bounds for the Extreme Value and Weibull Distributions.* Technometrics, v. 17, no. 2, May 1975.

values for failure data plus run-out values. The run-out values are non-failed bars with only the information that they have not failed at a specified number of cycles.

Using the QA data from GD it was determined that the maximum number of required cycles can be reduced to 110,000 as compared to the maximum of 570,000 currently being required to cause failure of the most durable bar. A comparison of material design allowable values obtained from both complete sample (all data) and censored data (only failed data below 110,000 cycles) showed excellent agreement. The allowable represents a value determined from a specified probability of survival with a 95% confidence in the assertion. Survival probabilities are 0.99 for the "A" allowable and 0.90 for the "B" allowable.

The above indicates that equivalent information could be obtained with a large saving in time while reducing fatigue machine failures. Figures 10 and 11 show the censored data results.

Metallurgical Evaluation and Other Mechanical Properties

A metallurgical evaluation was conducted on two failed M60 torsion bars, one produced by General Dynamics (GD) and the other by Machine Products Company (MPU). The parameters addressed in this evaluation are:

- o chemical analysis
- o light microscopy
- o retained austenite
- o hardness traverse-spline and body
- o tensile properties - room temperature (RT)
- o Charpy impact transition data longitudinal (LR) orientation
- o Charpy impact - (RT and -40°C), transverse (TR) orientation
- o fracture toughness (RT and -40°C) (LR and TR orientations)

Table 2 contains a near-complete chemical analysis for the GD material plus a carbon and sulfur content for the MPU product. As can be seen, the GD bar conforms to the specifications for AISI 8660, which is also shown in Table 2. It also meets phosphorus and sulfur requirements (0.040% each) in MIL-5-45387BAT.

Table 3 shows the results of a Rockwell C hardness (HRC) traverse in both a spline and body location for a GD material and the spline location for the MPU bar. It can be stated that both companies meet the hardness requirements of HRC 47-51 per MIL-5-45387BAT.

Tensile data from the GD bar are shown in Table 4. Duplicate tests were conducted and the data are consistent.

Longitudinal and transverse Charpy V-notch energy data are tabulated in Table 5. Longitudinal tests were conducted over the temperature range of +240°C to -40°C and transverse tests at +22°C and -40°C. A comparison of the data at room temperature and -40°C shows that the longitudinal energy values are superior to those of the transverse orientation. Values are 7.7 and 5.5 ft-lb and 2.7 and 2.9 ft-lb, respectively.

Fracture toughness data (K_Q) are tabulated in Table 6. These values were obtained using slow bend specimens at room temperature and -40°C in both an LR

and TR orientation from a GD bar and room temperature TR orientation from an MPU bar. Room temperature LR values are higher than TR, 43 versus 38.3 ksi$\sqrt{in.}$ GD TR data is slightly higher than MPU, 38.3 versus 34.2 ksi$\sqrt{in.}$ Two short rod tests were conducted on MPU material with resulting average K_Q value of 35.5 ksi$\sqrt{in.}$

Microstructural and retained austenite studies were also conducted on the GD material. The microstructure consisted of tempered martensite and 3% or less of retained austenite.

IV. FAILURE ANALYSIS

In addition to the metallurgical investigations which were performed on failed torsion bars, fractographic examination was also performed. One of the basic principles of failure analysis is the preservation of the fracture surface in a condition as close as possible to that at the time of failure. Another principle is the compilation of historic data concerning the failed component. The first principle issue was not achievable since the available torsion bars were found in scrap bins at either the depot or testing grounds resulting in fracture surfaces with some rust on them. The second issue was resolved by using a statistical model for the random loading spectrum, this will be discussed later.

Figures 12a through 12d show typical field failures which were obtained from Anniston Army Depot, APG, Ft. Knox and GD, which exhibited similar failures. They obviously initiated within the splines at the ends of the bar, and in most cases at the wheel arm end. One exception is a case observed at APG where the failure was at the anchor block end. These observations are supported by case studies obtained from the Measurement and Analysis Division at APG[5] and GD.[6]

Light microscopy and scanning electron microscopy (SEM) were used in the examination of the fracture surfaces. The failed bar in Figure 12a was cut open and examined. The arrow shows the origin of the fracture. The arrow on Figure 13a shows the surface of the serration which experienced surface plastic flow at the initiation site. This indicates high stresses at the inner end of the splines. There is a slight indication of fatigue marking in Figures 13b and 13c, but not as large as usual. The SEM examination (Figure 13d), however, did not show the usual striation beach marks associated with fatigue crack growth. This indicated that once fatigue crack initiation occurred, the propagation stage was very short. Further away from the initiation site, the fracture surface showed signs of corrosion and hydrogen embrittlement. It should be noted here that the fracture surface was old and could have been contaminated by the environment after failure.

V. STRESS ANALYSIS

The stress analysis of the splines was performed to evaluate various probable modes of failure. For the spline teeth, the possible modes of cracking are longitudinal, inclined, and transverse, with respect to the axis. Such cracks (Figure 14) are associated with various stress states, where the predominant ones are torsional

5. Aberdeen Proving Ground Report, Case Nos.: 78-M-4 - *Comparison Test of M60A1 Rise Tanks;* 79-M-9 - *Comparison Test of M60A1 Rise Tanks;* 80-M-34 - *Failure Analysis of M60A3;* 82-M-57 - *Analysis of Torsion Bar Spring Failures;* and 82-M-32 - *Failure Analysis of Two M60A3 Torsion Bar Springs.* Measurement and Anal. Div., Phys. Test Branch, STEAP-MT-G, Aberdeen Proving Ground, MD
6. *Rebuilt Tank Reliability Analysis.* General Dynamics, Land System Div. M60, MG-80-01731-006, March 1982.

shear stresses, Hertzian stresses, and bending stresses. These stress states are three dimensional in nature and therefore the analysis could be very expensive unless some simplifications are made. Three types of stress models were chosen to simplify the problem. The final results were then combined and used in the failure evaluation.

Bearing Stresses on Spline Teeth

Due to the existence of a missing tooth in the spline, it is suspected that the highest stressed area in bearing would be in that location. The bearing stresses were evaluated assuming that the load on the missing tooth is distributed equally on both neighboring teeth (Case 1) or only on the forward tooth (Case 2). The analysis was carried out using substructuring and superposition of the two load cases.

The stresses produced by the contact forces depend on the number of teeth in contact, and the distribution of contact force along the teeth. The number of teeth in contact depends on the tolerances, misalignment and load, while the distribution of the contact force depends on the teeth shape and moments of inertia of the axle and block. Figure 15 shows the finite element model used. Figures 16 through 21, the stresses in ksi resulting from bearing forces are shown.

Torsion of Nonuniform Bar

The enlargement of the ends of the torsion bar leads to stress concentrations at the fillets. The solution of this problem was carried out using the finite element method; a heat transfer analogy of the classical Michell torsion problem. Appendix A gives the details of the thermal-mechanical analogy and the boundary conditions used in the analysis. The finite element mesh and the results in ksi of this analysis are shown in Figure 22.

Evaluation of Stress Intensities

Four crack locations were considered in the fracture analysis:

1. Surface crack in the shaft (Mode III)
2. Subsurface crack in the shaft (Mode III)
3. Surface crack in the spline area away from the missing tooth (Modes I and III)
4. Same as 3, but at the missing tooth (Mode I)

The Mode I analysis used the results of the finite element model in Figure 15. Mode III results in ksi of Cases 1 to 3 were obtained by the solution of a St. Venant problem (Figure 23). The finite element penalty method was used for the multiply connected region case of subsurface cracks (see Appendix B). In all the above fracture analyses the quarter-point crack tip elements were used.[7]

Redesign - Reduction of Stresses in Spline

As demonstrated from the failure analysis and from the bearing stress and fracture analysis, the splines are the most highly stressed region in the torsion bar. A reduction of the contact stresses can be accomplished through a more uniform distri-

7. BARSOUM, R. S. *On the Use of Isoparametric Finite Elements in Linear Fracture Mechanics.* Int. J. Num. Meth. Eng., v. 10, 1976, p. 25-37.

bution of the stresses by redesigning the splines. Figure 24a shows the bearing stress distribution from current spline design (uniform teeth). Using tapered teeth permits intentional redistribution of the contact stresses between the splines and end blocks. From the deformation of the splines, as determined by the finite element analyses in section V - Bearing Stresses on Spline Teeth and Torsion of Nonuniform Bar - it was calculated that a 0.005 in. tapering increases the contact zone and reduces the maximum bearing stresses by more than 25% as shown in Figure 24b. Machining of such tapered teeth is accomplished using a gear shaper.

VI. SIMULATION PROCESS AND RELIABILITY EVALUATION DUE TO RANDOM LOADING

Random Loading - Amplitude Displacement Model

There is a lack of load spectrum data for the M60 tank. The only available data was that of an M1 tank test conducted at APG is shown in Figure 25. The test track contained a series of artificial ramps and bumps (Belgium blocks), to simulate a specific test course (Figure 26).

The angular amplitude distributions of three bars from these tests is shown in Figure 27. The positive and negative angular displacements of the bars as a function of tank travel are shown in Figure 27a. The zero angular rotation is referenced to the static deflection of the torsion bar and hence does not give zero stress in the bar. Figure 27b shows the amplitude distributions in a manner describing percent time less than a specific value [positive sign (+)] and percent time greater than a specific value [negative sign (-)], e.g., 25% level equals a -75% level. The positive peak represents maximum angular displacement under load; the negative peak is the maximum rewind angular measurement. The range of angular rotation is defined as follows:

$$\Delta\theta = \theta + |\theta^-|$$

where θ^- = maximum negative angular displacement, and (1)

θ = displacement from Figure 27.

The Beta distribution provided the best representation of the skewed amplitude distribution. The dampening effects that occurred under load resulting from a stop used in preventing further angular twist of the bar produces highly skewed discrete cumulative probability values. The Beta function is defined as:

$$f(\Delta\theta) = \frac{\Gamma(P+Q)}{\Gamma(P)\Gamma(Q)} (\Delta\theta)^{P-1} (1-\Delta\theta)^{Q-1} \qquad (2)$$

$$0 \leq \Delta\theta \leq 1 \quad P,Q>0$$

The P and Q values are selected in a manner that provides the best probability density function (PDF) for representing the data. Figure 28 describes a typical distribution and Table 7 shows the excellent fit between predicted (Beta representation) and actual test results. As shown in the fatigue analysis, section VI, Fatigue Life - S/N Curve Analysis, angles less than 20° represent stresses sufficiently low that infinite torsion bar life could be expected, therefore, a good representation below this angle is not essential.

Figure 29 shows a typical load spectrum result of an M60 A3 torsion bar. The results were obtained for a DADS* simulation process performed at TACOM. A stochastic model was introduced in order to simulate the bar response. The spectrum is represented by positive and negative angular displacements versus time, as shown. Included in the figure are tabulated absolute amplitude values using Equation 1.

The uniform probability density function was selected to represent the amplitude distributions. The selection process involved evaluating an informative quantile (IQ) plot[8] of the amplitude data. In Figure 30a, the IQ plot of data tabulated in Figure 29 is shown. The straight line represents an exact uniform distribution with the disjointed line representing actual data. Figure 30b is a schematic of a typical distribution model for DADS simulation data.

Fatigue Crack Growth Law for Estimating Torsion Bar Life

Initial efforts in applying the Monte Carlo method for determining reliability versus cycles to failure of the torsion bar involved using the crack propagation laws. The da/dN data requires extensive testing, time, and material. For this reason, and due to the short life expended in crack propagation because of the operating stress levels, it was decided to rely on published results. As shown in Figure 31, the percentage of life spent in initiating and propagating a crack depends on the stress level and material toughness. The da/dN relationships for materials metallurgically similar to the specified AISI 8660 material were obtained from References 9 through 11, and are shown in Figure 32. The dry air results made available by Barsom[10] provided the most representative estimates of crack growth versus stress intensity (ΔK) since the torsion bar is protected from the environment. It is to be noted that the mean stress effect was ignored in this analysis. From the basic da/dN relationship, N cycles to failure as a function of crack growth, angular displacement, and the geometry of the region where the crack initiates in the bar may be obtained from the following relationships:

$$N = \int_{a_i}^{a_f} \frac{da}{0.66 \times 10^{-8}\ \Delta K^{2.25}} \qquad (3)$$

where $\Delta K = A_j \Delta\theta \sqrt{\pi a}$

with A_j's (see below) representing the stress intensity multiplier associated with each configuration of the cracks discussed in the previous sections. The $\Delta\theta$ is the range of angle of twist.

A_1 = 4.91 (missing spline tooth)
A_2 = 3.29 (other spline regions)
A_3 = 3.26 (torsion bar body).

*DADS is a vehicle dynamics computer simulation program used by TACOM's concepts lab. It should be noted that the authors are not convinced that the M60 suspension system is accurately represented in the DADS program. Therefore, the results in Table 9 should not be taken as absolute values, but as demonstrations of the methodology.

8. PARZEN, E. *Entropy Interpretation of Tests for Normality by Shapiro-Wilk Statistics.* Presented at the Twenty-Eighth Conference on the Design of Experiments in Army Research, Development and Testing, Monteray, CA, 20-22 October 1982.
9. *Damage Tolerant Design Handbook.* Metals and Ceramics Information Center, Battelle Columbus Laboratories, MCIC-HB-01, 1975, p. 8.2-D.
10. *Damage Tolerant Design Handbook.* Metals and Ceramics Information Center, Battelle Columbus Laboratories, MCIC-HB-01, 1975, p. 8.2-E.
11. BARSOM, J. M. Transactions of ASME. J. of Eng. for Ind., Series B, v. 93, no. 4, November 1971.

The range in stress intensity factor ΔK was calculated by combining Modes I and III at locations 1 and 2 on the spline (see section V, Evaluation of Stress Intensities) through the use of the strain energy release rate definition. The fracture toughness in Mode III was taken to be $\sqrt{(1 - \nu^2)/(1 + \nu)}$ multiplied by the Mode I toughness.

Note, a percent reduction in a_i's will provide a decrease in the stresses in the specific region of the torsion bar. The a_i and the a_f parameters are initial and critical crack size, respectively. The a_f is obtained from the critical stress intensity value K_{IC} for the material considered, 36 ksi $\sqrt{in.}$ in this case. The angular displacement of a bar $\Delta\theta$ can also be represented by the equvalent stress range as

$$\begin{aligned} \Delta\tau &= rG\,(\Delta\theta)/L \text{ where} \\ r &= \text{radius of shaft,} \\ G &= \text{torsional modulus,} \\ \Delta\theta &= \text{angular rotation range, and} \\ L &= \text{length of torsion bar.} \end{aligned} \tag{4}$$

The Monte Carlo Process

Crack Propagation Analysis

A schematic of the Monte Carlo process is outlined in Figure 33 for determination of frequency of occurrence versus cycles to failure of the torsion bar using the crack propagation law. An assumed normal distribution is used to represent variability in the A_j, a_i, and a_f parameters. A coefficient of variation (CV) defined as:

$$CV = \frac{SD}{mean} \tag{5}$$

establishes the standard deviation (SD) for the corresponding known mean value (e.g., a_i for initial crack size). Coefficient of variation values of 5, 10, and 15 percent were considered in developing the distributions in order to examine the effects of variability (inherent errors in measurements, flaw size assumption or the stress analysis) in the parameters. By selecting the above CV's, a sensitivity analysis can be developed, thereby providing a method for recognizing the importance of the parameters as related to the cyles to failure. The $\Delta\theta$ Beta distribution, as shown in Figure 33, has been previously defined in Equation 2.

The random numbers used in the Monte Carlo process are obtained from solving for X in

$$\int_{-\infty}^{x} f_i \, dx = R \tag{6}$$

where R is a uniform random number and f_i corresponds to the desired type of frequency distribution for the parameter. A probability density function for the N cycles to failure can be obtained by randomly selecting discrete sets of numbers from the a_i, a_f, A_j and $\Delta\theta$ distributions and substituting them into Equation 3. Note, there should be an equal amount of random numbers for each parameter to have the proper amount of numbers for the N distribution.

Fatigue Life - S/N Curve Analysis

Torsional bar life expectancy was obtained using the Monte Carlo process applied to the S/N curve relationship. The above procedure provided a method for obtaining lifetime estimates of the bar by combining the effects of crack initiation and propagation. A description of the S/N curve is given in Figure 34, where the base line data was obtained from a literature survey for material metallurgically similar to the torison bar material. The survey provided a set of S/N curves for torsional fatigue, shown below, for best representing the current materials used in the bar.

$$\mathrm{Log}_{10}N = B + 0.068\ \Delta\theta \tag{7}$$

where B = 7.70 for base line data.

The slope value of 0.068 was essentially the same for all curves in the set. The adjustment in B from 7.70 to 8.06 is made on the basis of M60 torsion bar quality assurance tests at a single $\Delta\theta$ value performed at the Scranton manufacturing facility (see Figure 6). A single load equivalent to a 42^o angular displacement was applied during the quality assurance torsional fatigue test. Use of the mean value and the cycles to failure in Figure 6 provided a more accurate estimate of B. The curves representing a range of 10 and 20 percent reduction in bar stress are also shown in Figure 34.

The S/N curve Monte Carlo process is similar to the previously outlined method for da/dN relationship. The primary difference involves using models for B and $\Delta\theta$ from Figures 34 and 27, respectively. A schematic of the basic S/N representation is shown in Figure 35a. The simulation of S/N curve variability is shown for a specific value in Figure 35b. Figure 35b also describes the probability density function (PDF) for B. A random selection of a discrete set of numbers from $\Delta\theta$ and B distributions is then applied to Equation 7 in order to obtain the $\mathrm{Log}_{10}N$ value. The process is repeated until all values from the two distributions are selected. This process will then provide a PDF to represent $\mathrm{Log}_{10}N$. Again, in the S/N evaluation, the mean stress effect was ignored for torsional loading.[12]

Torsion Bar System Reliability

By assuming a tank with m torsion bar systems, the following procedures would be applied in order to establish the reliability of the system. After the reliability for each torsion bar failure is calculated, the next task is to determine the overall suspension system reliability.

If all of these torsion bar failures are independent of each other then the system reliability R_S would be given by

$$RS = \prod_{i=1}^{m} R_i \tag{8}$$

where R_i = reliability for torsion bar i, i = 1, 2,....,m, and m = total number of torsion bars in the suspension system.

12. FORREST, P. G. *Fatigue of Metals.* Pergamon Press, New York, 1962, p. 103.

If these torsion bar failures are not independent of each other, then the system reliability would be given by

$$R_S = R_1 \times R_2/R_1 \times \ldots \times R_m/R_{m-1}/\ldots/R_1 \tag{9}$$

where

$$R_m/R_{m-1}/\ldots/R_1$$

is the reliability of torsion bar m, given the reliabilities of m - 1 ..., 1 bars.

It should be noted here that the reliability of the individual bars R_i is different due to the difference in load spectrum it experiences.

Remaining Life - Reliability of Operation After Specific Number of Cycles

When the torsion bars of a rebuilt M60 tank are reused in service after a Depot inspection, one would assume that a specific number of cycles on the bars could be found. Currently, no information is recorded and, hence, the following is a hypothetical evaluation. The reliability of operating an additional number of cycles when a specified number of cycles of operation has been completed is obtained in the following manner. Initially, it is assumed that a specified distribution function such as f(N) is known, for example, the distribution of $\mathrm{Log}_{10}N$ from the Monte Carlo method previously described. The reliability $R(n_1, n)$ is a conditional probability requiring the probability of operating for $(n_1 + n)$ cycles when n_1 cycles have been completed. That is,

$$R(n_1,n) = \frac{R(n_1 + n)}{R(n_1)} = \frac{\int_{n_1+n}^{\infty} f(N)dN}{\int_{n_1}^{\infty} f(N)dN} \tag{10}$$

where n is the additional mission in cycles after n_1 cycles of operation. the number N_s (n_1, n) of components (torsion bars) that will survive additional n cycles is given by

$$N_s\ (n_1\ n) = N_s(n_1) \cdot R(n_1\ n) \tag{11}$$

where $N_s(n_1)$ = number of components starting the mission of n additional cycles.

Results of the Reliability Study

The proper number of simulations for the Monte Carlo method depended on the models under consideration. For example, 5000 and 3000 were required for the da/dN and S/N curve models, respectively. Using a convergence rate criterion for the calculated one percent values [P_s (see Figure 36)] and recognition of the third and fourth moment stability of the $\mathrm{Log}_{10}N$ distribution provided an excellent method for determining required number of simulations. Differences in percentile values

for coefficient of variation (CV) of 10 and 15 percent were minimum for da/dN simulation of parameters. The 10 percent value was used for all da/dN calculations.

The torsion bar reliability results from the da/dN relationship are given in Figure 37. The current design results were obtained from Equation 3, with A_2 = 3.29, which represents the stress state in the spline region. They indicated a relative limited lifetime range of 14 to 500 miles, with probability of survival (PS) values of 0.99 and 0.01, respectively. An appropriate increase in a_f (final crack length) from Equation 3 represents the 40% increase in the K_{IC} value. This represents an improvement in the material's capability with respect to acceptance of larger flaw sizes prior to failure. The slight improvement in the bars capability indicates that an improvement in material will not significantly improve bar performance. The 25% and 50% reduction in K_I (stress intensity) in Figure 37 is obtained from reducing A_2 in Equation 3 by the respective percentages. These reductions represent improvements in the design of the spline section of the bar as shown in Figure 24. The K_{III} failure in the shaft represent situations where failure occurs in the shaft rather than in the spline region.

The maximum life of 70 miles at 25 mph achieved from a 50 percent improvement in spline design with a 0.99 probability of survival indicates that there is very limited life of the bar after crack initiation. Table 8 describes minimum life estimates (99 percent survivability) for crack, e.g., propagation of the torsion bar with respect to various tank velocities and the design improvements. Tank travel at 5 mph (lowest speed) with a 50% reduction in K_I value shows propagation life expectancy of only 341 miles at 0.99 probability of survival.

The failure probability obtained from the S/N curve - Monte Carlo application is shown in Figure 38. The resultant exponential form is consistent with that expected from the S/N model in the analysis.

A graphical display of PS versus miles to failure is shown in Figure 39 for the 25 mph tank velocity. The life expectancy of the bar is much greater than that obtained from the da/dN analysis. The minumum life estimate (0.99 PS) of 292 miles is 21 times greater than the 14 miles determined from the da/dN results for crack propagation. This result indicates that most of bar life occurs prior to crack initiation. Therefore, the torsion bar should be manufactured in such a manner that flaws are minimized. The current shot peening used in the manufacture of the bar indicated recognition of this fact by the manufacturer. The bar reliability estimate obtained after an assumed 741 miles of tank travel are shown in Figure 39. The increase of the probability of survival from 0.90 to 0.99 if the bar survives the initial 741 miles does not provide a sufficient gain to warrant reusing bars since the minimum increase in expected life is reduced very rapidly. The results (Table 9) for a 20 percent reduction in design stress gives 865 miles for a PS of 0.99. This is a considerable improvement when compared to that of 292 miles for the current design. The results from velocity ranging from 5 mph to 25 mph in increments of 5 mph are given in Table 9 with respect to current 10 and 20 percent improvements in design. Reducing velocities of tank operation obviously improves reliability of the torsion bar.

It should be noted that the field test data used in the comparison with the reliability calculation refers to the failure of the first (or front) torsion bar. The front wheel arms have a different suspension system than the rest of the wheel arms, and hence the spectrum of loading on the torsion bars is quite different. They

are subjected to higher loads and have a higher incidence of failures. The same reliability calculations can be performed on the other bars in order to calculate the reliability of the system (Equations 8 and 9).

Examination of current design mileage capability of the bar for 20 and 25 mph indicates a range from 276 to 292 miles. These results agree with the 262-mile minimum life obtained from Aberdeen Proving Ground (APG) test results, Table 10 (taken from Reference 13 of bar failure from 3-mile test course), which are represented in the probability distribution of Figure 40. This course and tank velocity were similar to those used in obtaining the load spectrum results. The excellent agreement between the predicted and actual life expectancy of the bar indicates the desirability of the Monte Carlo process for modelling variability of loads spectrum (design stress) and S/N curve (material capability) results. Table 10 gives the failure results of tests run at APG. The failure life of the torsion bars are in agreement with the above predictions.

Although excellent agreement has been obtained, the authors would have preferred representing the spectrum load consistent with an individual peak-to-peak angular displacement. The simplification applied using the negative peak as base and representing the displacement relative to this value was a good approximation to the available individual displacements. This approximation would provide a slightly conservative estimate in the reliability values. Using the ASTM recommended pratice of representing the lower of 3 times the standard deviation band of the S/N curve as a measure of material fatigue loading capability combined with maximum angular displacement (46 degrees) for 25 mph, a minimum life estimate of 112 miles resulted for the bar. Selecting this number as a design value could result in an overly conservative estimate, since chance that this maximum displacement could occur together with the S/N curve as the actual lower band, described above, is extremely small.

A minimum life of 575 miles was obtained by using the maximum displacement value with the original S/N curve where B = 8.06. This result is obviously wrong since in the limited samples of 23-bar failures, two of them failed at mileage less than 400 miles (see Figure 40).

Results from the application of the Monte Carlo process for DADS simulation data is shown in Table 11. The PS percentages and their corresponding miles of tank travel are tabulated for road arms 1L, 2L, and 6L at 5, 18, and 25 miles per hour. The APG12 course (18 mph) was the most severe according to the TACOM representative. The results from Table 11 reflect this, since the 0.99 percent PS of 14 miles was the lowest obtained from any of the computed life estimates at that PS value.*

Since this course introduces unusually large angular displacements of the bar 1L (see Figure 29) and requirements are only one failure in a hundred, this is not an unrealistic estimate of bar life. It is obvious from examination of Table 11 that road arm 6L will survive much longer than either 1L or 2L. Traveling at 5 mph in such a severe course will also increase bar life considerably.

*See footnote on page 7.

13. Aberdeen Proving Ground Report, Case No. 82-M-37, MT-5376, Aberdeen Proving Ground Test Branch.

VII. NONDESTRUCTIVE TESTING CONSIDERATIONS

Review of torsion bar field failure reports and examination of a number of fractured bars clearly illustrated that fatigue failures predominately initiate in the spline ends rather than in the reduced cross-section central gage length. Based on these data, it was initially considered that a periodic magnetic particle inspection for fatigue cracks in the spline surfaces would provide a technique for predicting premature failures. However, results of the subsequent fracture mechanics analysis reported herein have identified the critical crack size as 0.019 inch. Furthermore, the analysis shows that an existing fatigue crack, 0.005 inch deep, will propagate to critical size within only a few miles. Therefore, if a fatigue crack equal to or less than 0.019 inch exists, failure is imminent.

Figures 41a and 41b taken from Reference 14, show that a fatigue crack in steel must be greater than 0.030 inch for a 90% probability of detection at 95% confidence using the conventional magnetic particle inspection method. Significantly smaller cracks are indeed detectable using the technique, but probability of detection will be low in a production environment, as illustrated in Figures 41a and 41b. Inasmuch as the torsion bar must be removed from the vehicle to conduct an inspection at some arbitrary time, detection of a crack less than 0.019 inch would be only by chance. It was therefore concluded that, in the case of the M60 torsion bar, even the most sophisticated nondestructive crack detection scheme will not provide an effective life prediction technique. Once a fatigue crack initiates and can be detected, service life of the torsion bar has essentially ended.

VIII. CONCLUSIONS AND RECOMMENDATIONS

1. A methodology for obtaining reliability of the M60 tank torsion bar subjected to cyclic random loads has been developed where probability of survival is represented as a function of miles of tank travel.

2. As discussed in Reference 15, the developed methodology can be applied to other structures with cyclic random loads.

3. The use of the method appears justified from recognition of the excellent agreement between predicted reliability estimates and those obtained from the actual bar life (miles to failure) experienced during the tank operation.

4. Determination of minimum bar life was 21 times greater from the application of the S/N curve model than that of the assumed da/dN model. This indicates that most of the bar life is expended in crack initiation.

5. Application of deterministic procedures [use of lower three SD bound for S/N curve (ASTM method) and mean S/N curve] provide over and under design value estimates respectively while the Monte Carlo method outlined in the text accurately describes acceptable design values.

14. RUMMEL, W., et al. *Detection of Tightly Closed Flaws by Nondestructive Testing Methods in Steel and Titanium.* Martin Marietta, Denver, CO, Final Report MCR-76-476, NAS 9-14653, September 1976.
15. BARSOUM, R. S., et al. *M60-Torsion Bar Reliability.* Army Symposium on Solid Mechanics, Newport, RI, October 1984.

6. Calculations show that redesigning of the bars to reduce the stresses increases the life considerably. A slight improvement of 20% is much more effective in increasing life than requiring a higher toughness in the material.

7. Explore the use of the torsion bar presetting operation at the depot as a proof test for reused bars, and follow it by 100% magnetic flux inspection. Also, explore reshot peening of the whole bar, or replacement of the pinion and anchor blocks at the depot.

8. Recommend revisions to MIL-S-45387A by requiring the use of aircraft quality material and including requirements for grain size, cleanliness, and Charpy V-notch impact energy for both room temperature and -40°C. Such would longer life.

9. For new bars, it is recommended that materials other than AISI 8660, such as AISI 4350 steel be considered. Also, induction hardening followed by shot peening should be explored. References 16 and 17 cover this issue to some extent.

IX. TECHNICAL GAPS

In addition to the above conclusions and recommendations the study uncovered the following "Technical Gaps" which have to be resolved in future studies of this type.

1. Actual load spectra - the load spectra on actual test courses and other field ıpplications is not available. The design of new or improved suspension syste ·ill require this knowledge.

2. Data from various manufacturers - torsion fatigue data was only available from GD. Other manufacturers and potential suppliers of torsion bars had no data. In addition, the form of the data generated needs to be modified based on modern statistical methods as discussed in his report.

3. In general, there is a lack of fatigue and fatigue crack growth data for materials used in torsion bars. In addition, environmental, finishing, and mean stress effects on fatigue life are very difficult to obtain.

4. The effect of shot peening and hardening on fracture and fatigue life needs an extensive study.

5. Currently, there are no NDE methods for detection of small cracks. Also, NDE methods for field inspections are needed.

6. In order that bars which exhaust their fatigue life can be retired, a method of mileage record keeping for every bar is needed (this could be expensive). Microprocessors or mechanical angular displacement accumulators would be helpful for such a task.

16. GIBSON, D., BOERMAN, G., and GORUM, A. *High Strength Torsion Bar Development for Army Applications.* Contract DAAG46-76-C-0074, FMC Corp., San Jose, CA, Final Report, AMMRC TR 79-5, January 1979.
17. *High Strength Steel Torsion Bars.* TACOM, R7D Tech. Report No. 12746, 30 May 1983.

7. Maintenance procedures need to be revaluated in lieu of failure life of the component. In addition, the interaction between various components should be considered in their retirement.

8. Introduction of the censoring process should be made in order to reduce the amount of fatigue cycles necessary for QA of the bars. This will reduce the cost and time in the testing process.

X. ACKNOWLEDGMENTS

The author would like to acknowledge the following people: BG C. B. Donovan (PM-M60 at time of study), R. DeGrout (TACOM-PM-M60), A. Cummings and COL J. Aljets (APG), H. Briggs (GD), G. Boerman (FMC), F. Bibb and J. Bennett (Anniston), J. A. Robinson and R. A. McKinnon (APG-MTD) and 1LT G. Jackson and R. Musseau (TACOM-Concepts Lab).

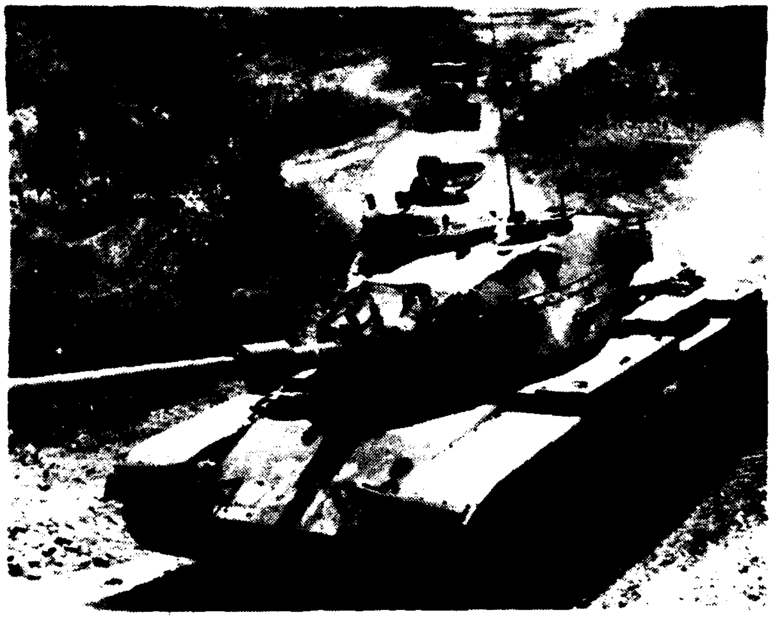

Figure 1. M60 tank.

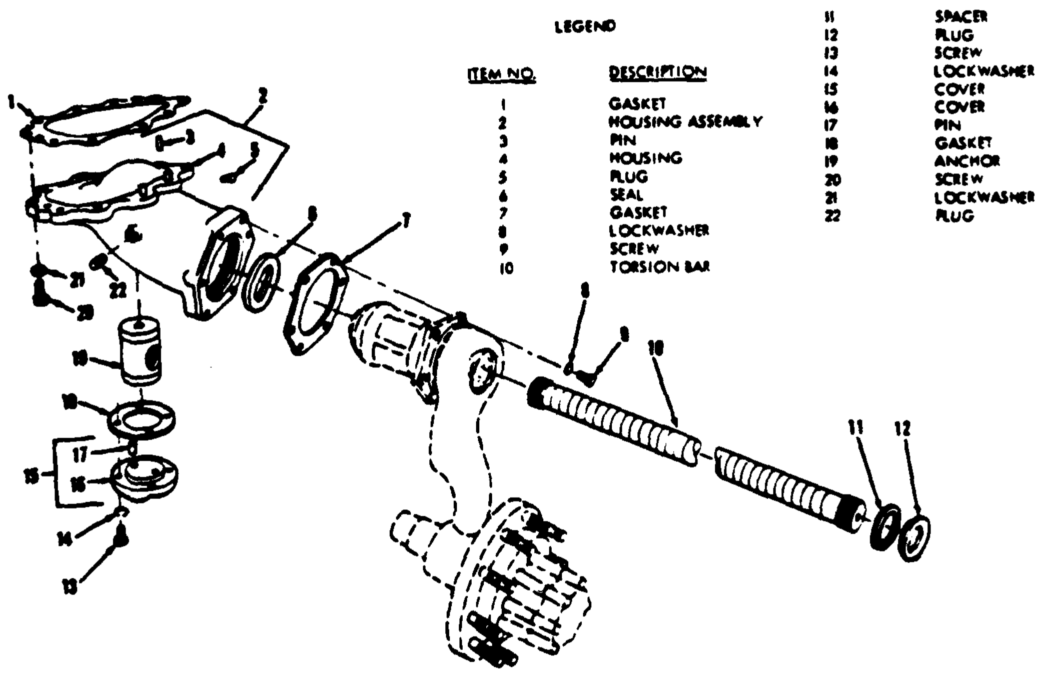

Figure 2. Numbers 1 through 6 roadwheel support housing, torsion bar, and related parts.

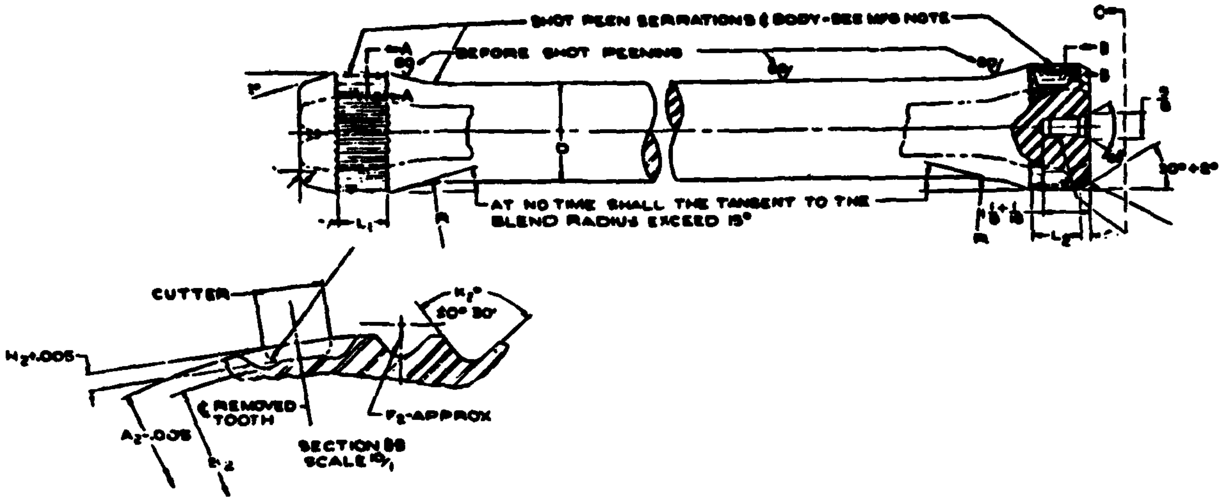

Figure 3. Torsion bar and teeth detail.

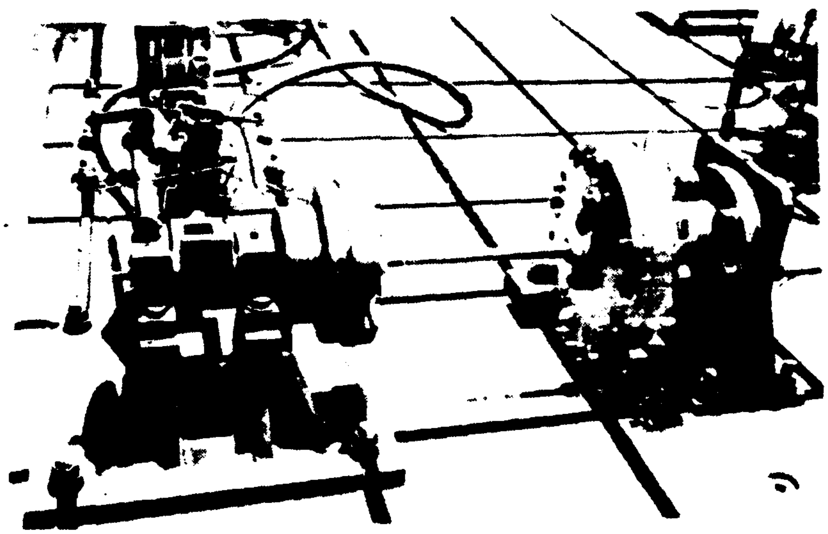

Figure 4. Torsion bar endurance test fixture (shown with scatter shield removed).

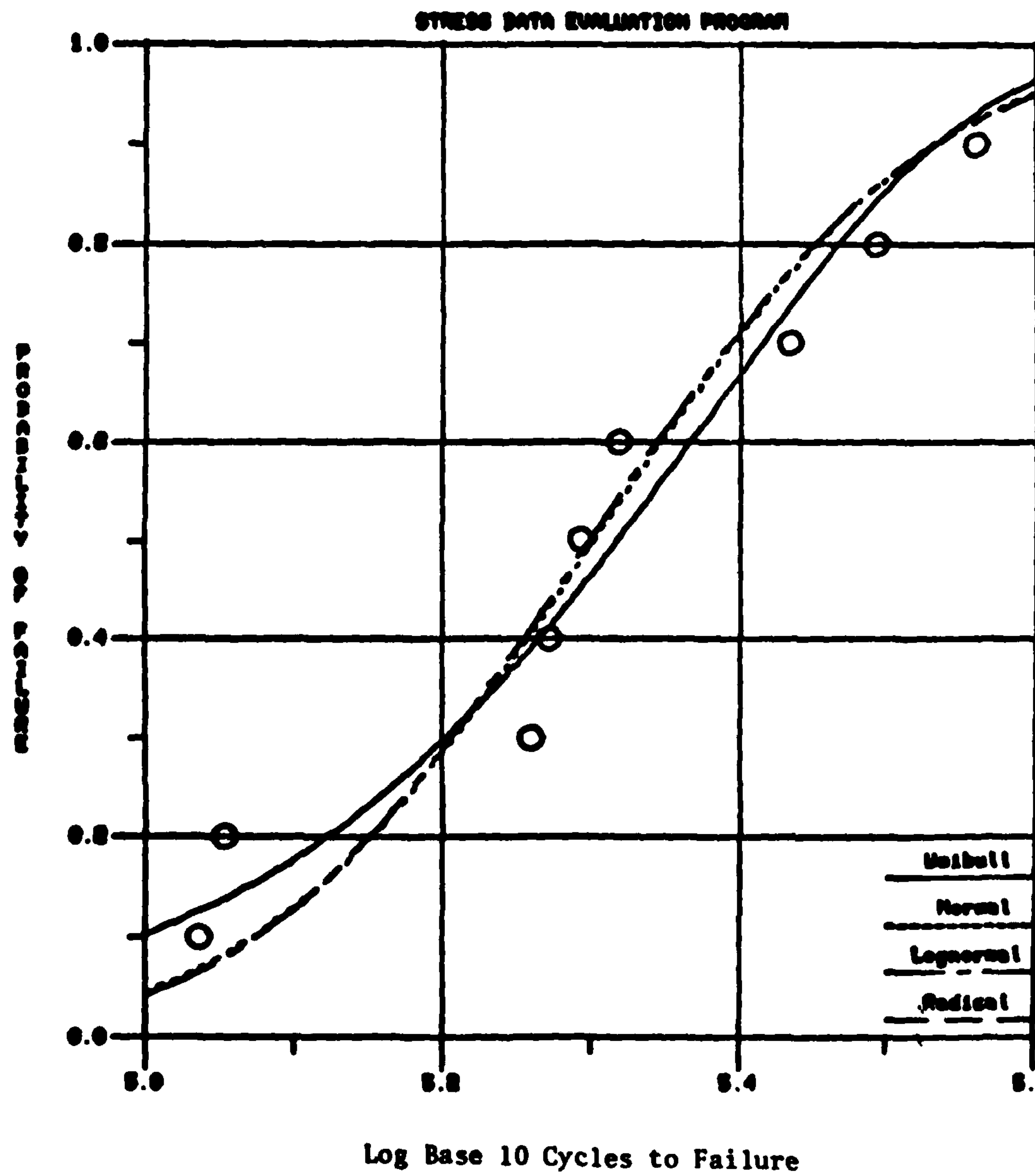

Figure 5. M60 torsion bar fatigue test results (1978).

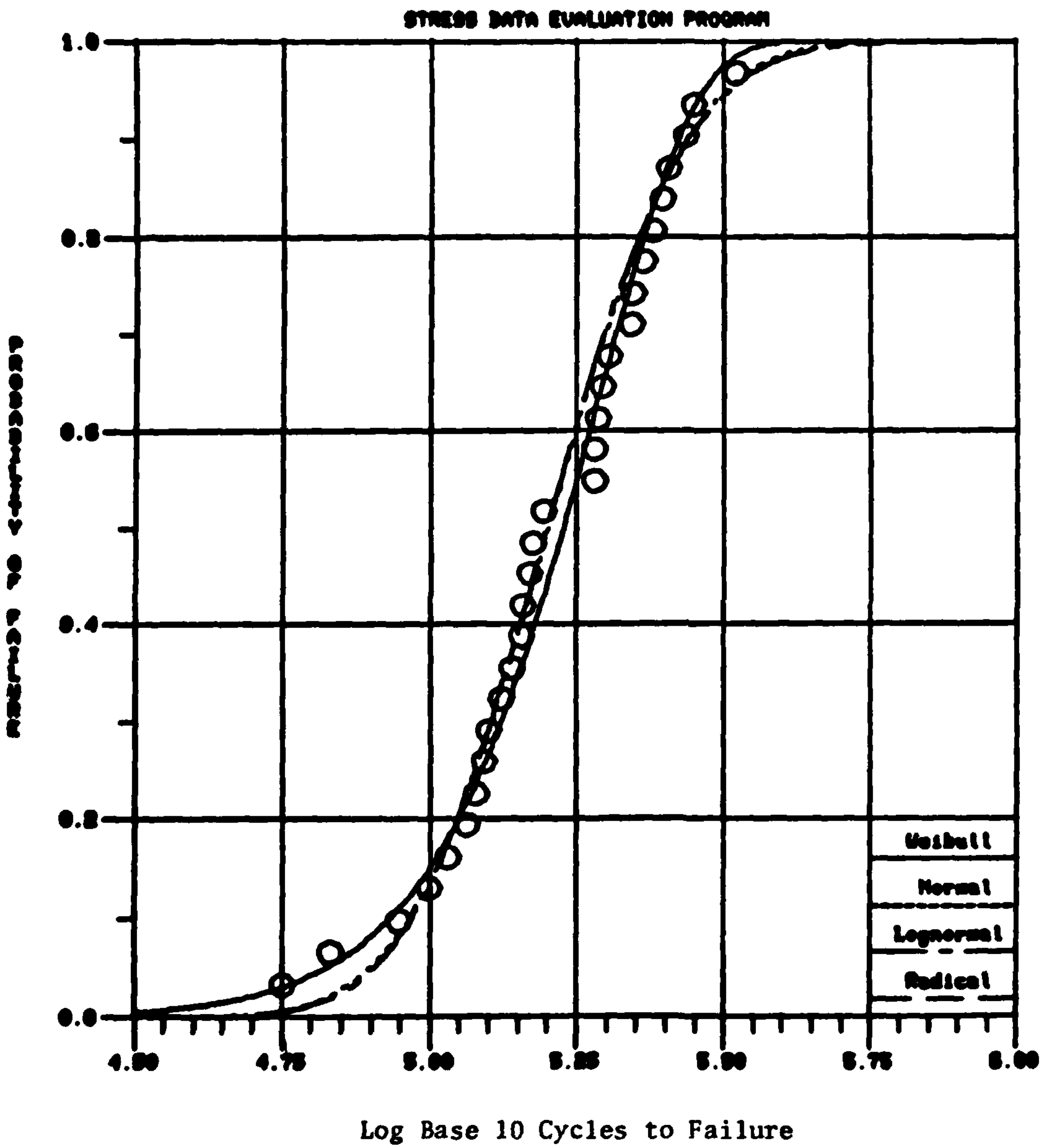

"A" Allowable Min. Life
25001 cycles (Weibull)
43551 cycles (Normal)

Figure 6. M60 torsion bar fatigue test results (1979).

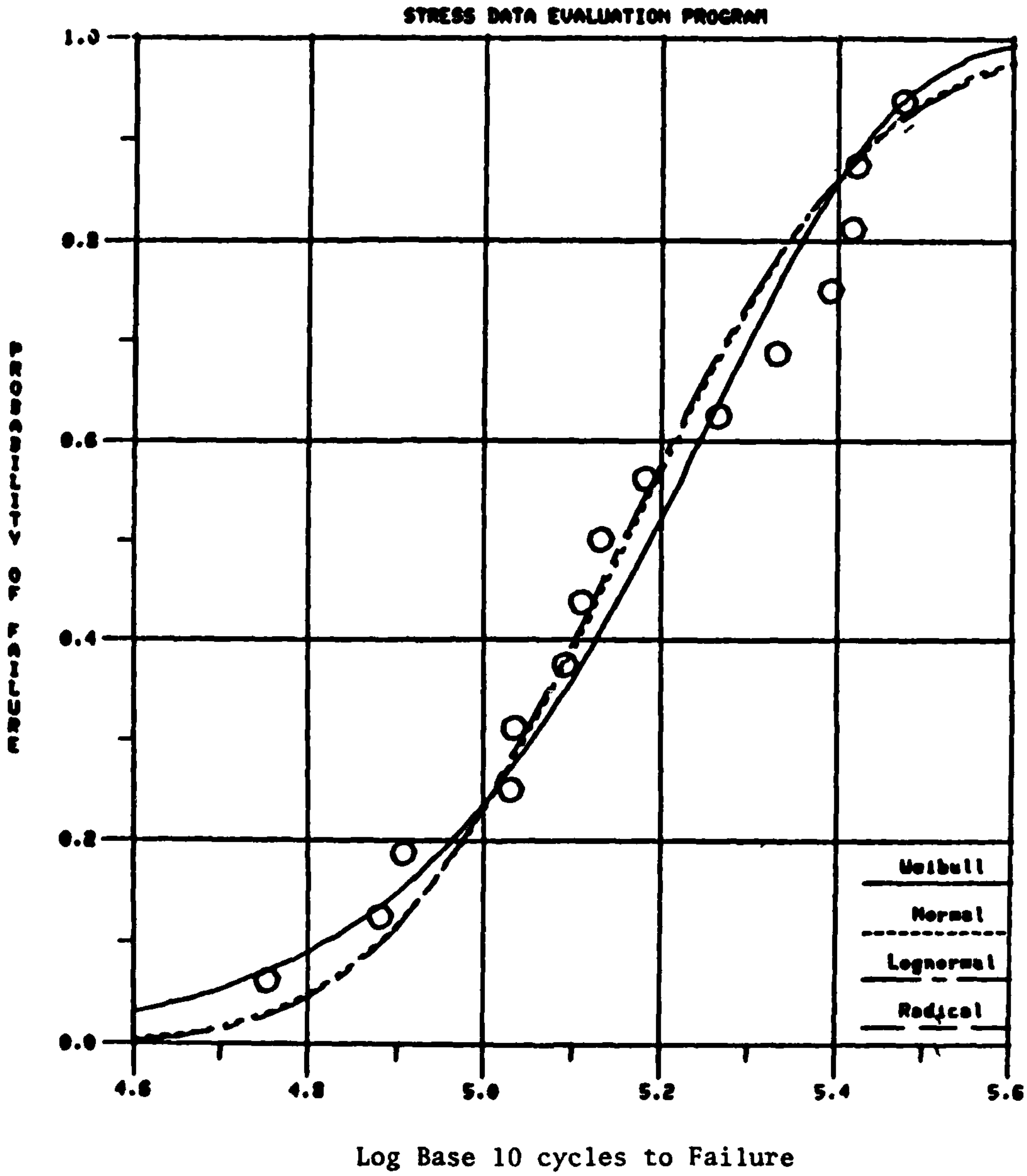

Figure 7. M60 torsion bar fatigue test results (1980).

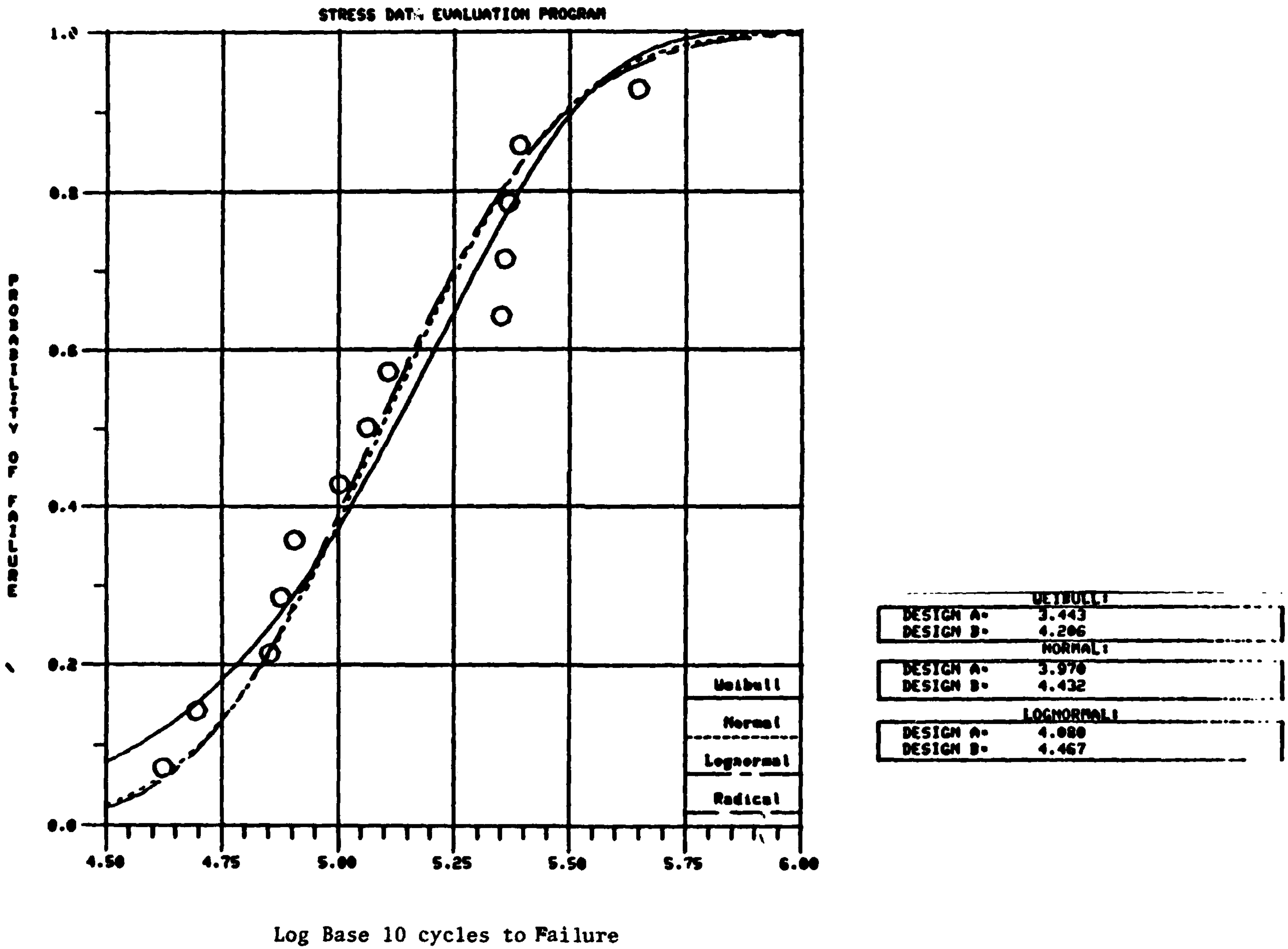

Figure 8. M60 torsion bar fatigue test results (1981).

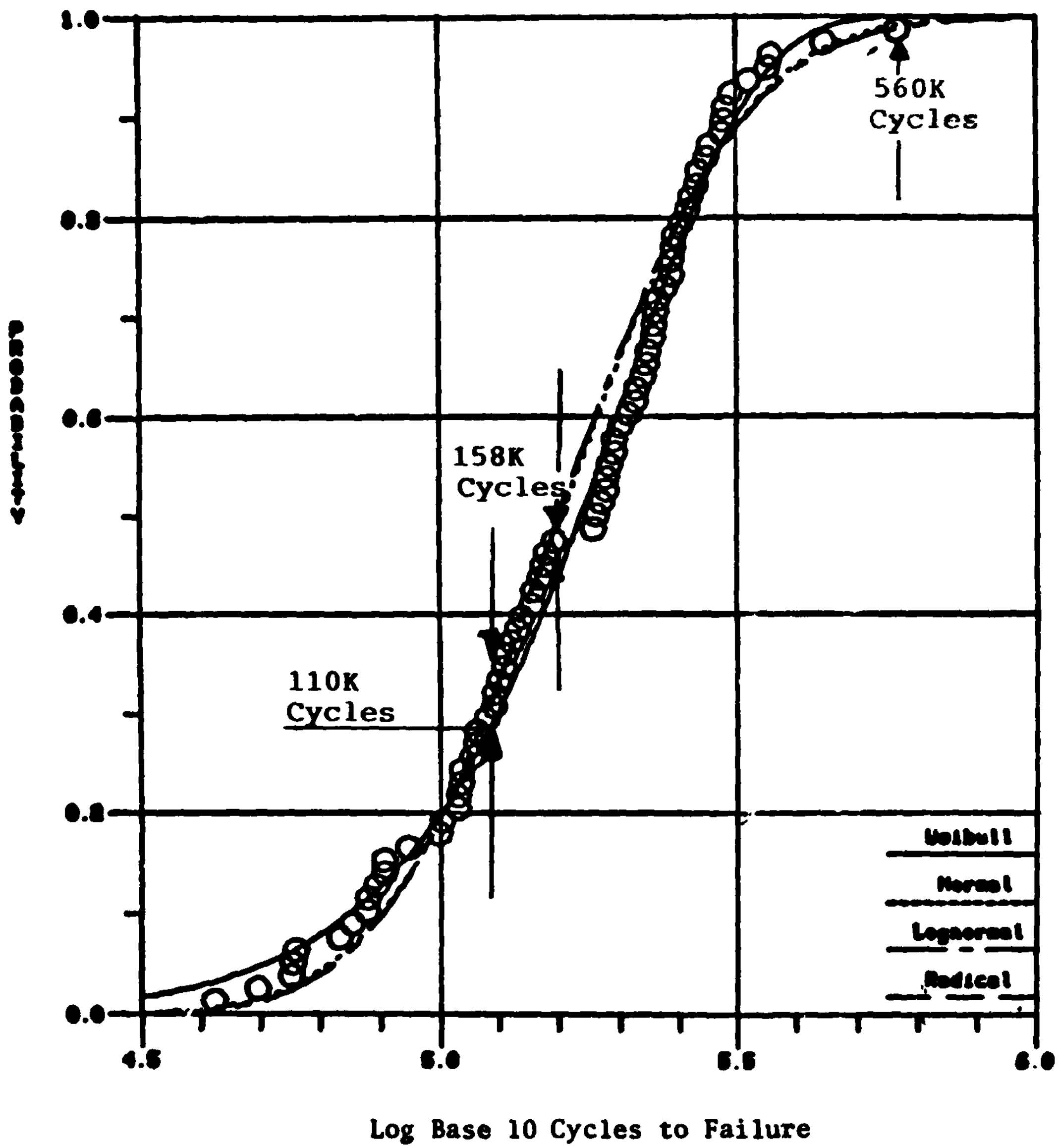

"A" Allowable Min. Life
18113 (Weibull)
35563 (Normal)

"B" Allowable Min. Life
57148 (Weibull)
67920 (Normal)

Figure 9. M60 torsion bar fatigue test results (pooled data 1977 to 1982).

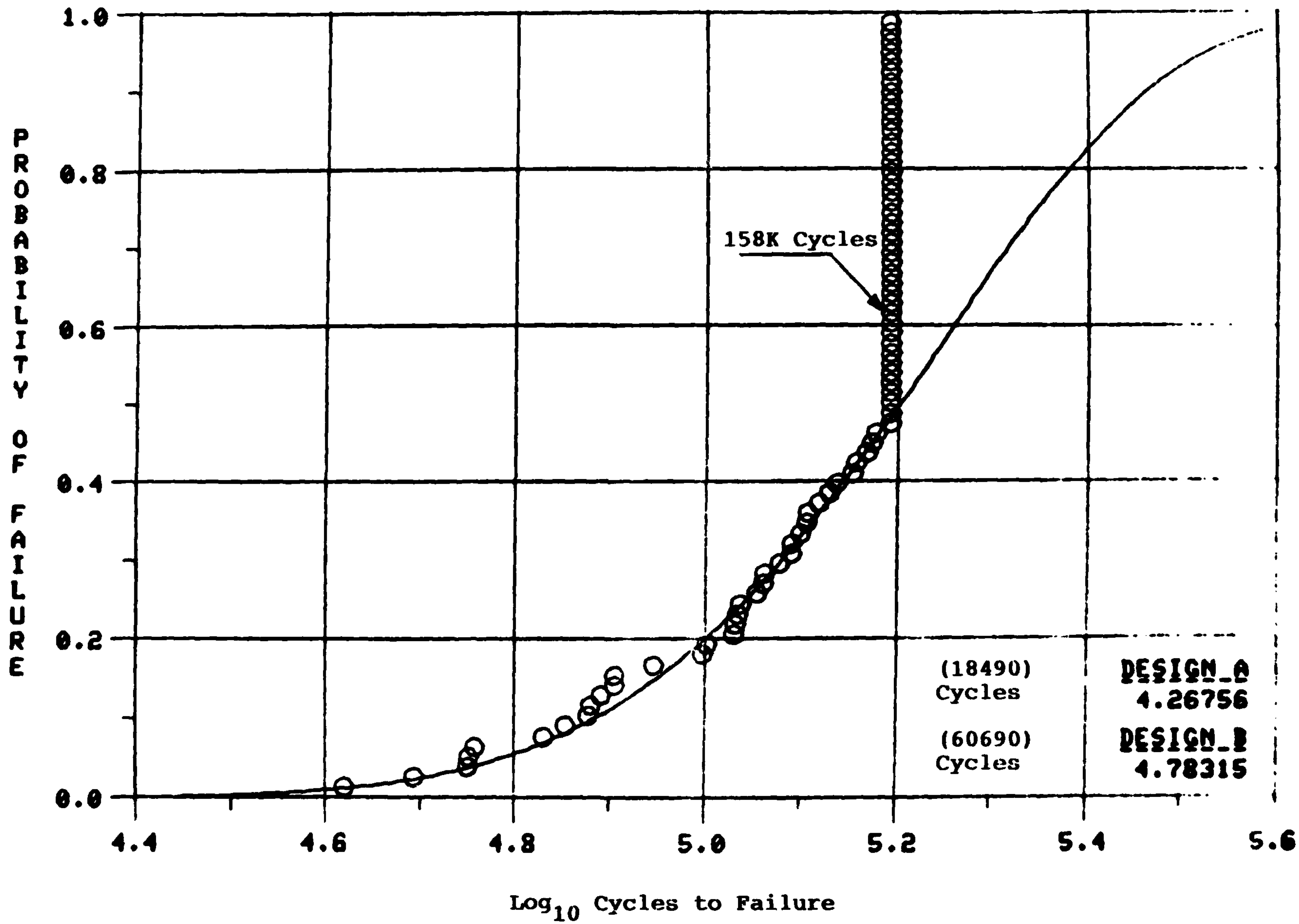

Figure 10. Weibull-censored data analysis of Scranton torsional fatigue test results.

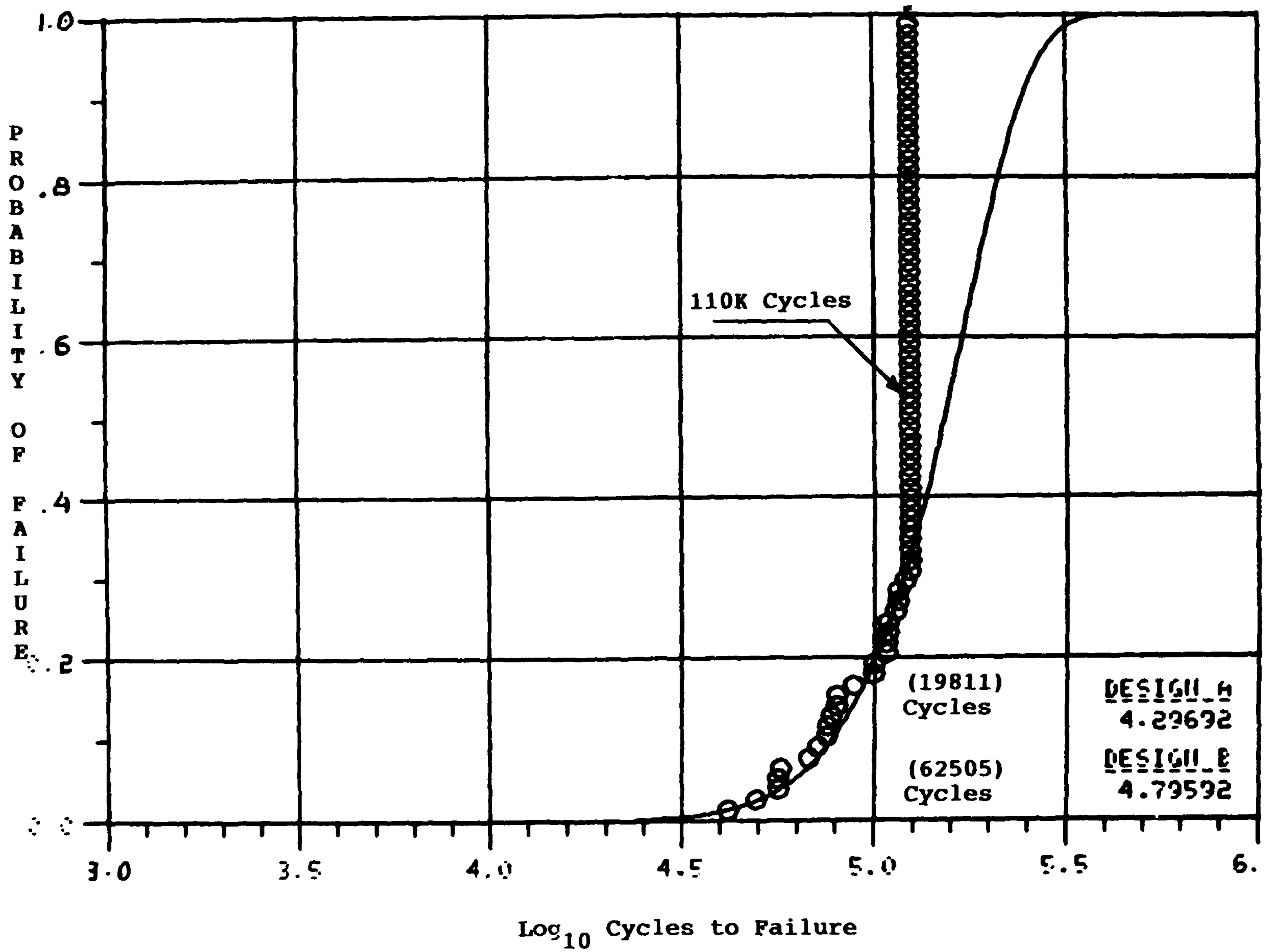

Figure 11. Weibull-censored data analysis of Scranton torsional fatigue test results.

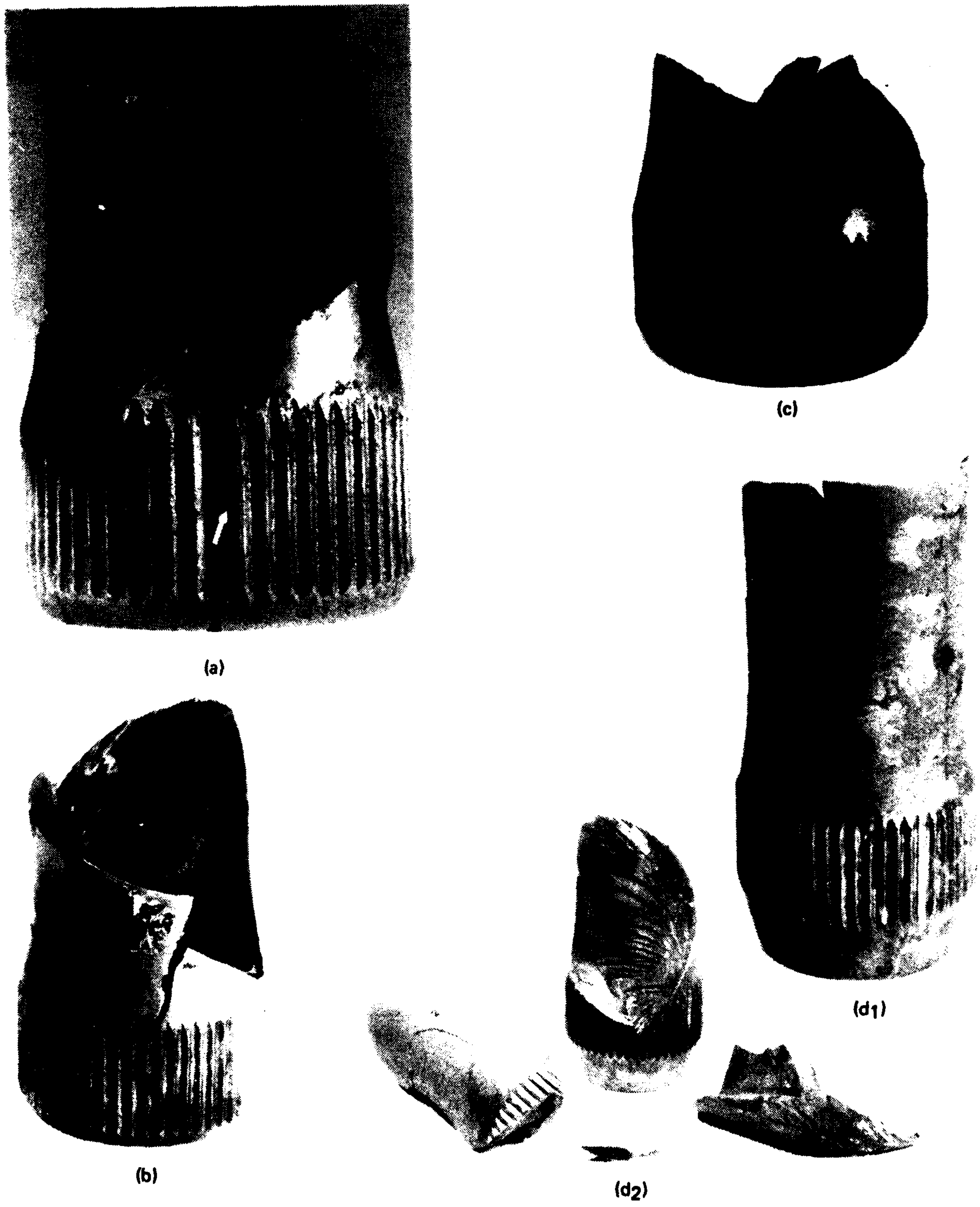

Figure 12. Typical field failures: (a-c) failure at wheel arm end, and (d) failure at anchor end.

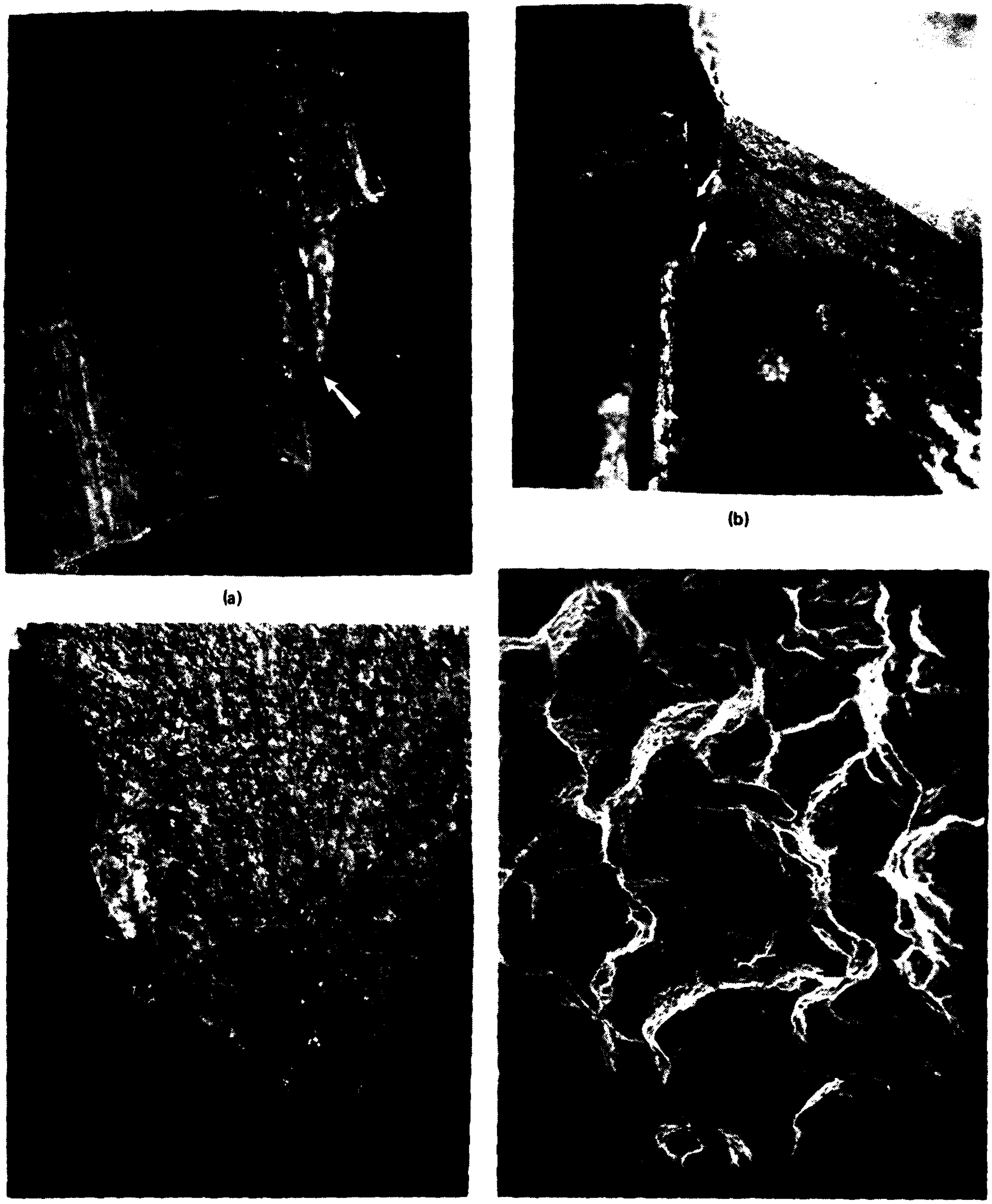

(a) (b) (c) (d)

Figure 13. (a) Plastic flow of teeth; (b) initiation site; (c) enlargement of initiation site; and (d) SEM - 1000X - corrosion.

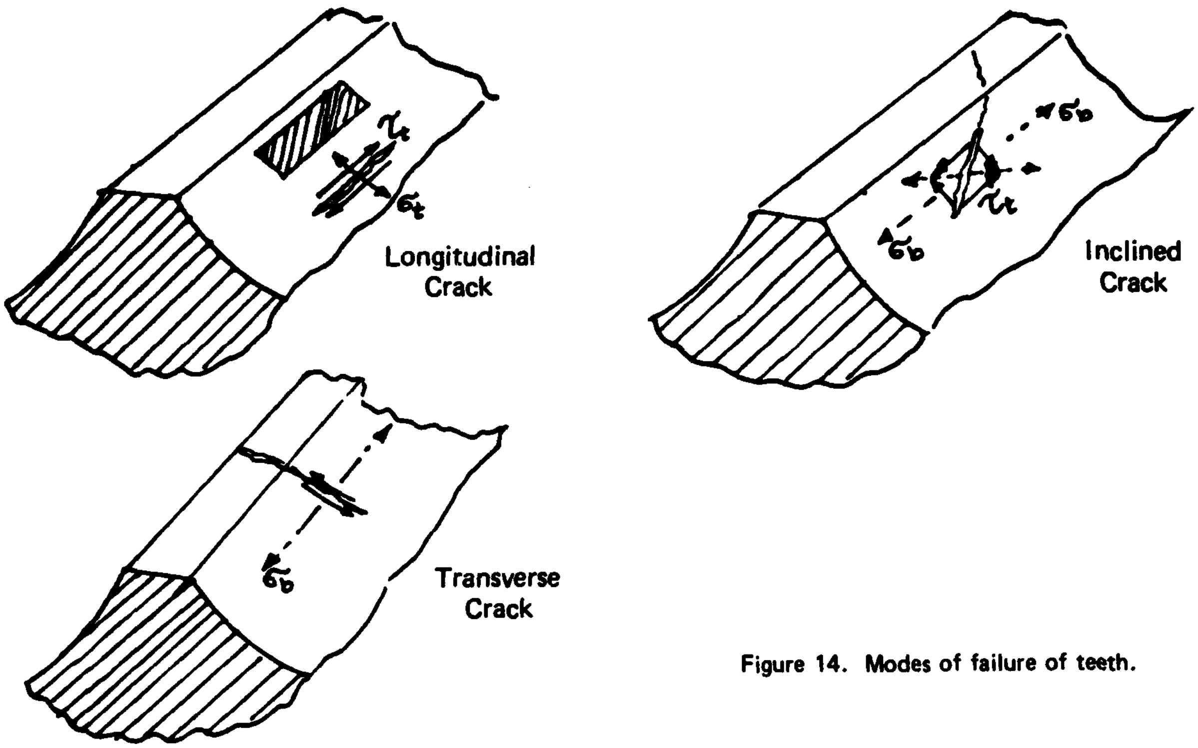

Figure 14. Modes of failure of teeth.

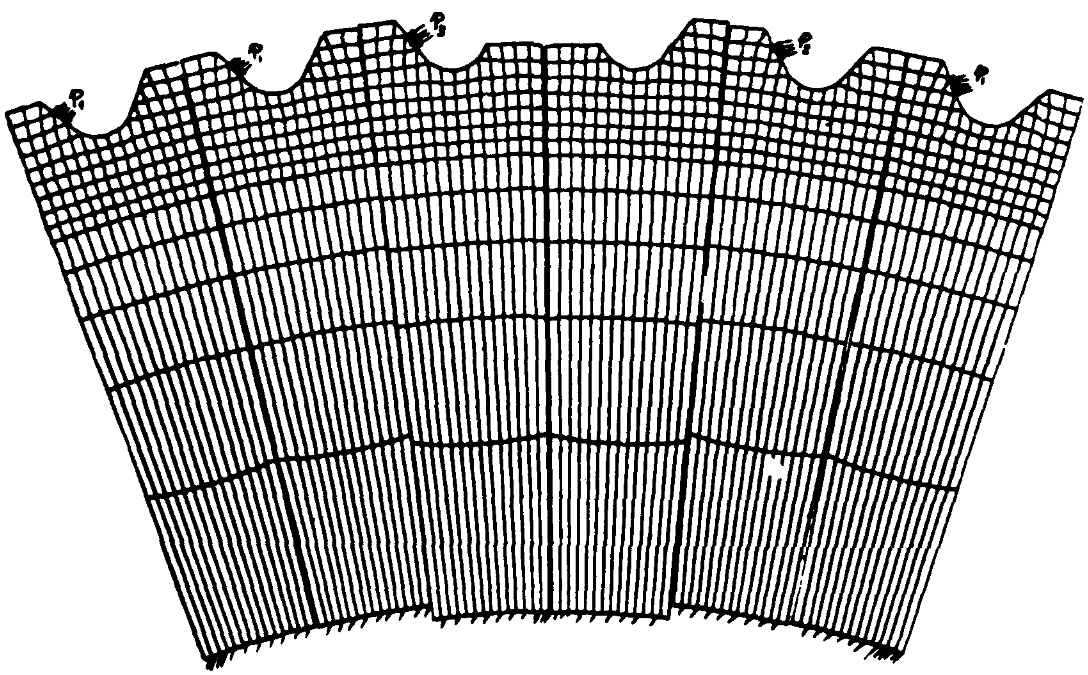

Figure 15. Finite element mesh for contact stress analysis:
Case 1 - $P_2 = P_3 = 1.5\ P_1$; and Case 2 - $P_2 = P_1$, $P_3 = 2\ P_1$.

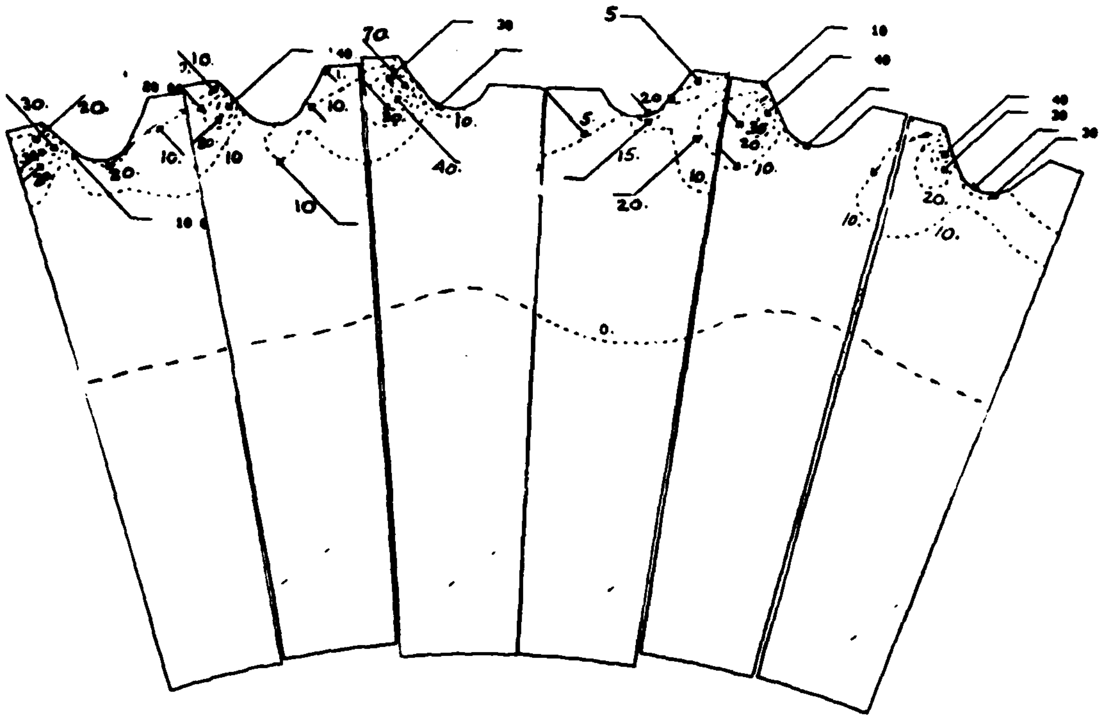

Figure 16. Contact stresses: effective stress contours Case 1.

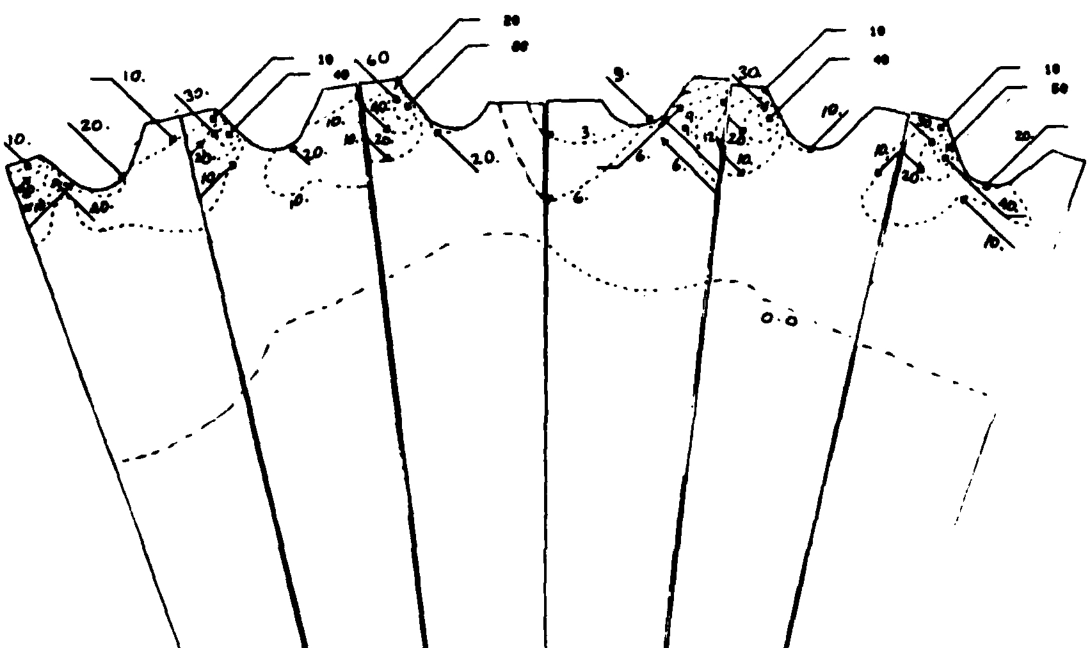

Figure 17. Contact stresses: effective stress contours Case 2.

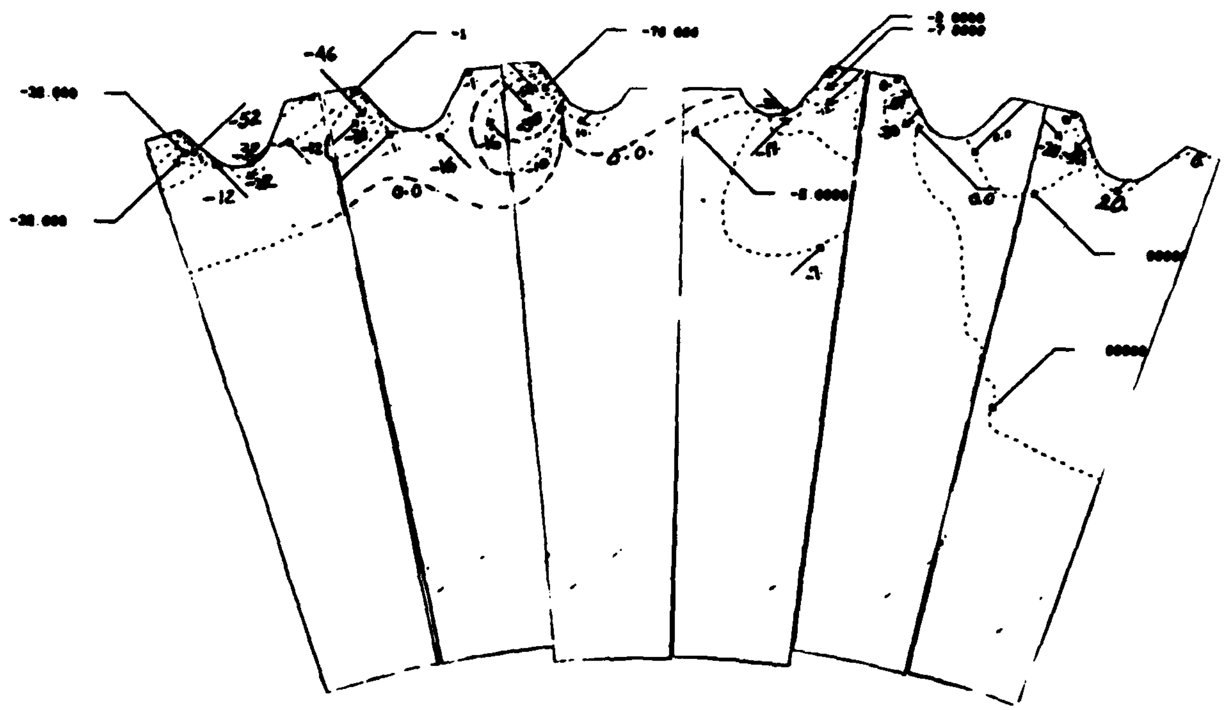

Figure 18. Contact stresses: maximum principle stress contours Case 1.

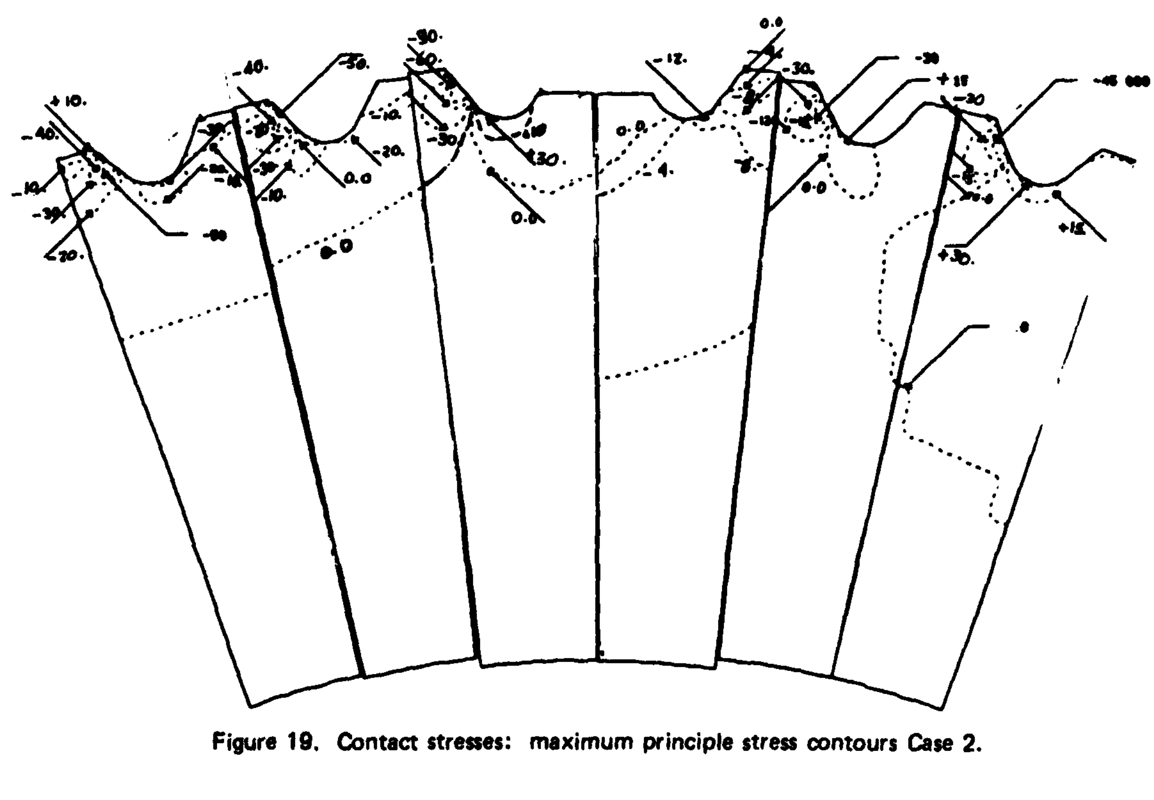

Figure 19. Contact stresses: maximum principle stress contours Case 2.

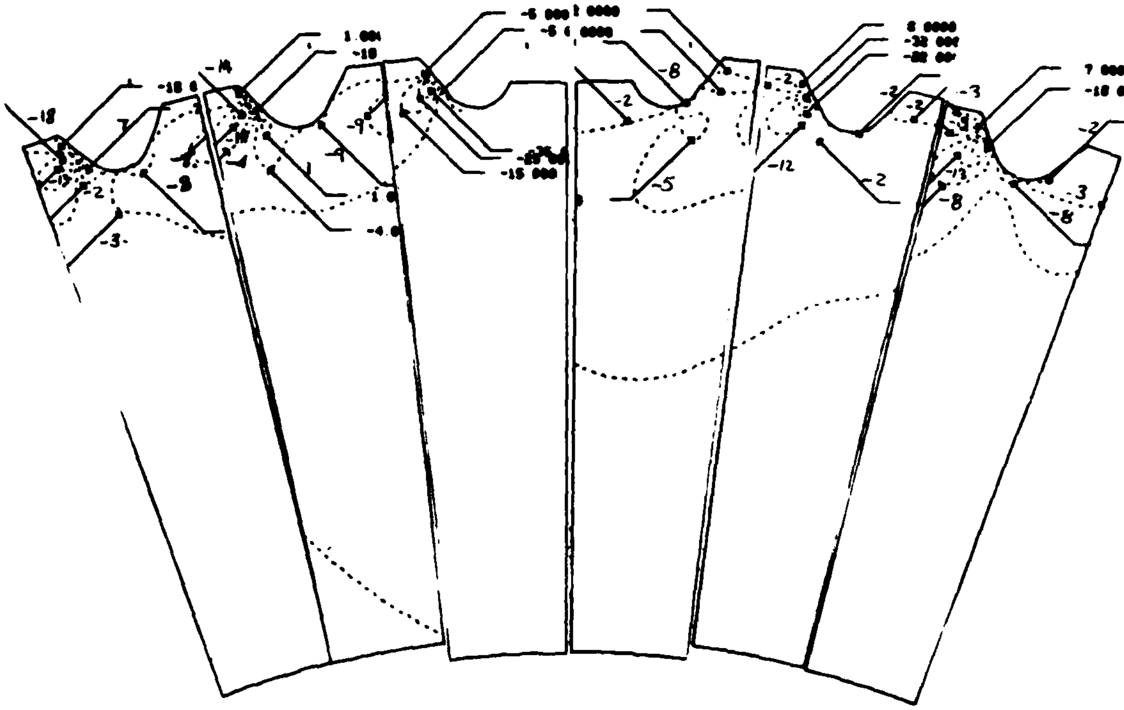

Figure 20. Contact stresses: shear stress contours Case 1.

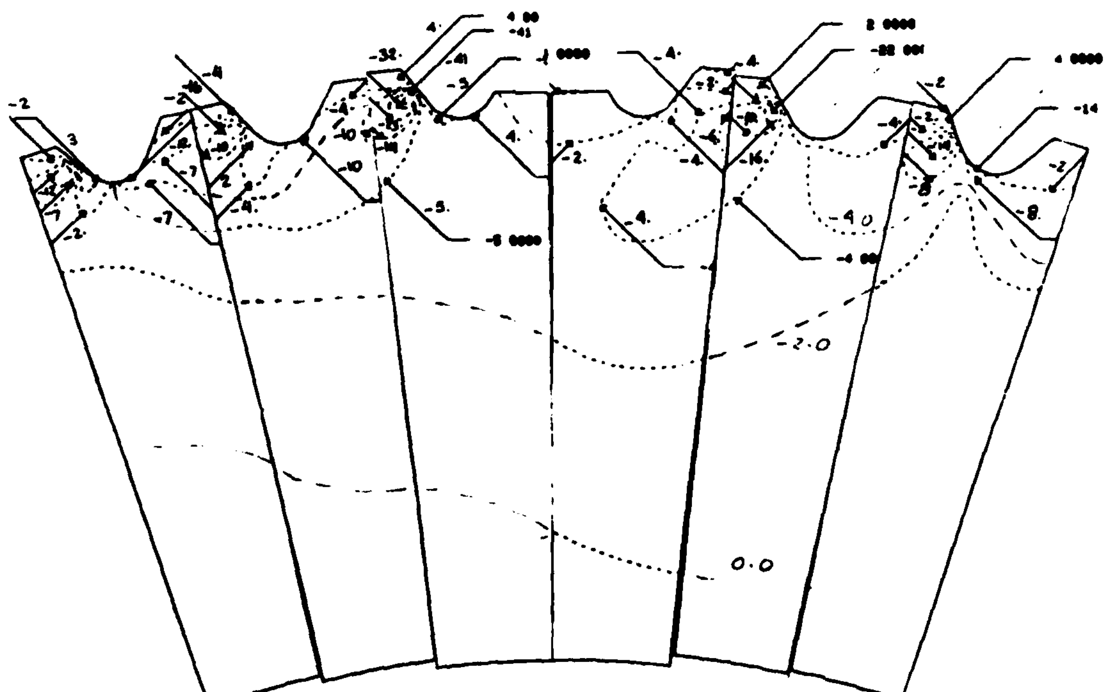

Figure 21. Contact stresses: shear stress contours Case 2.

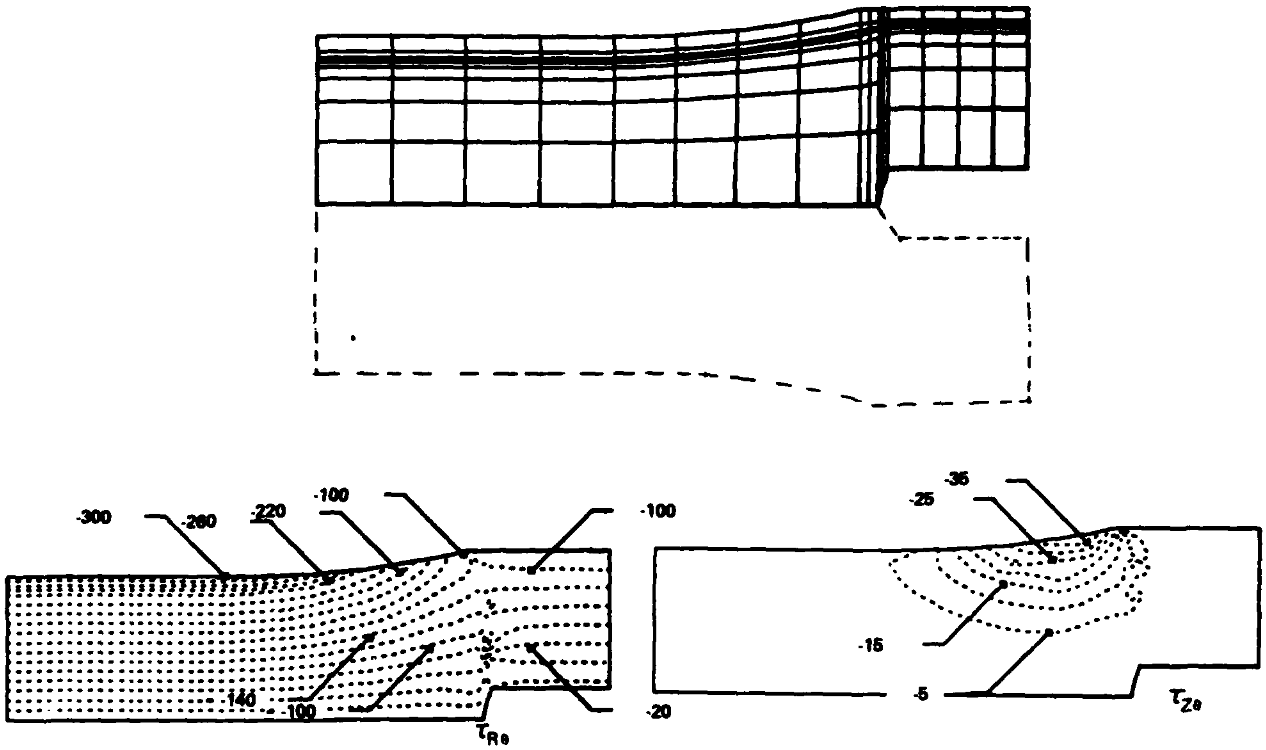

Figure 22. Torsional stresses at enlarged end of bar (Michell problem).

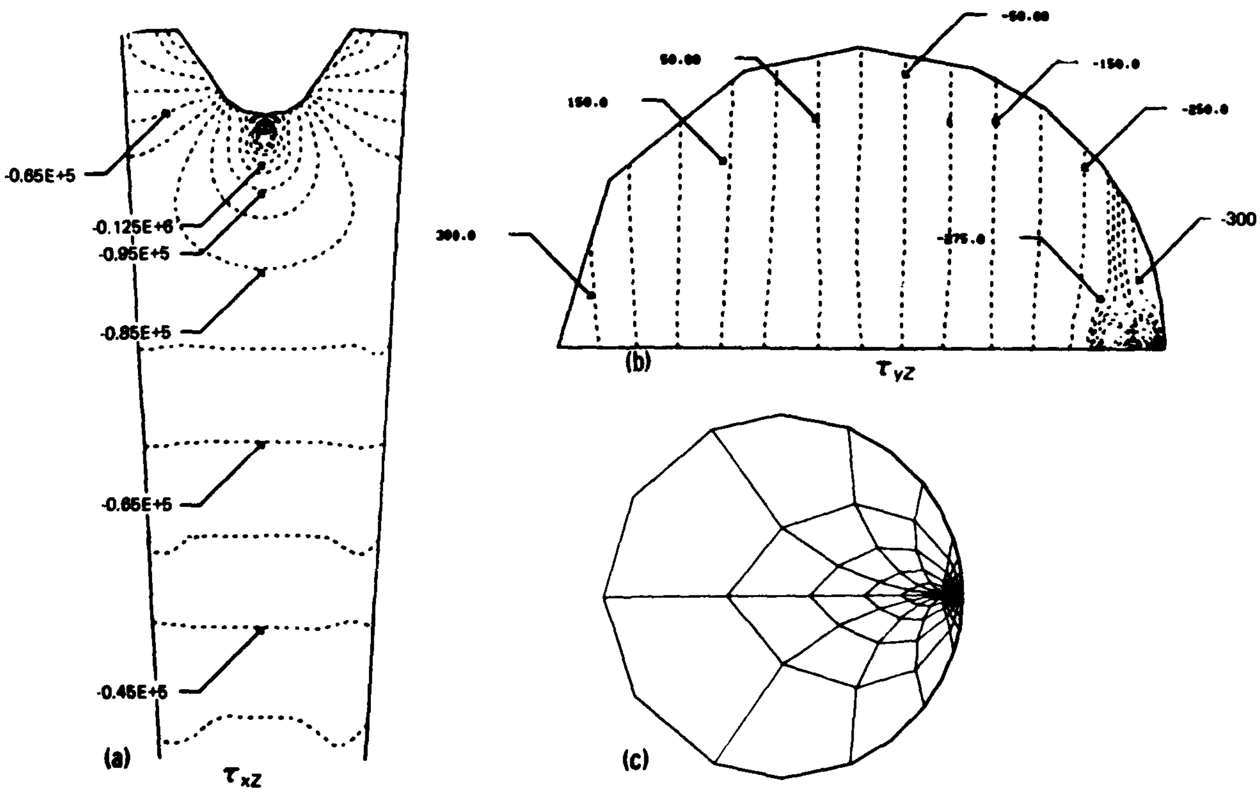

Figure 23. Torsional stresses Mode III; (a) cracked spline, (b) subsurface crack, and (c) finite element model for subsurface crack.

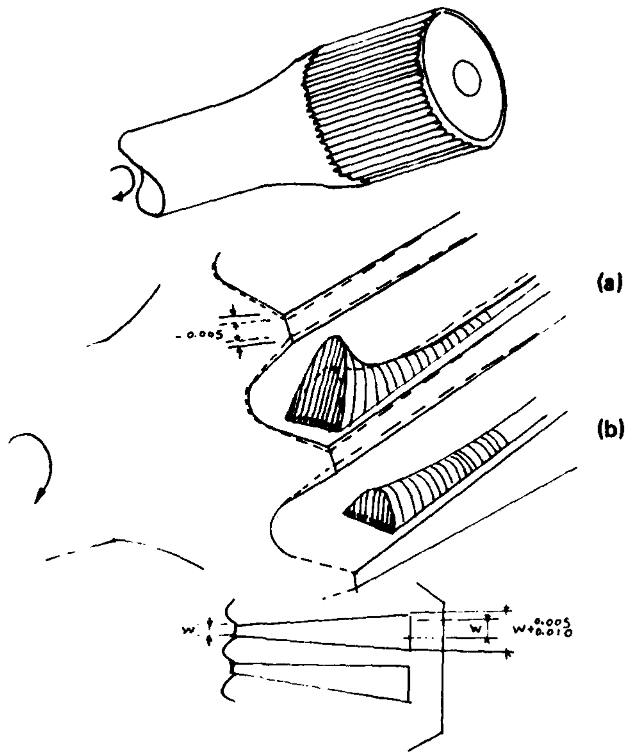

Figure 24. Stress distribution on spline teeth (effect of tapering).

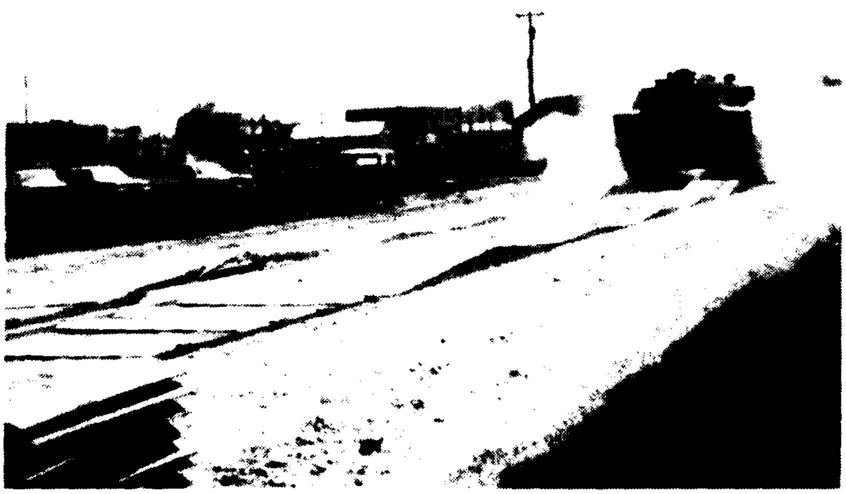

Figure 25. M1 test.

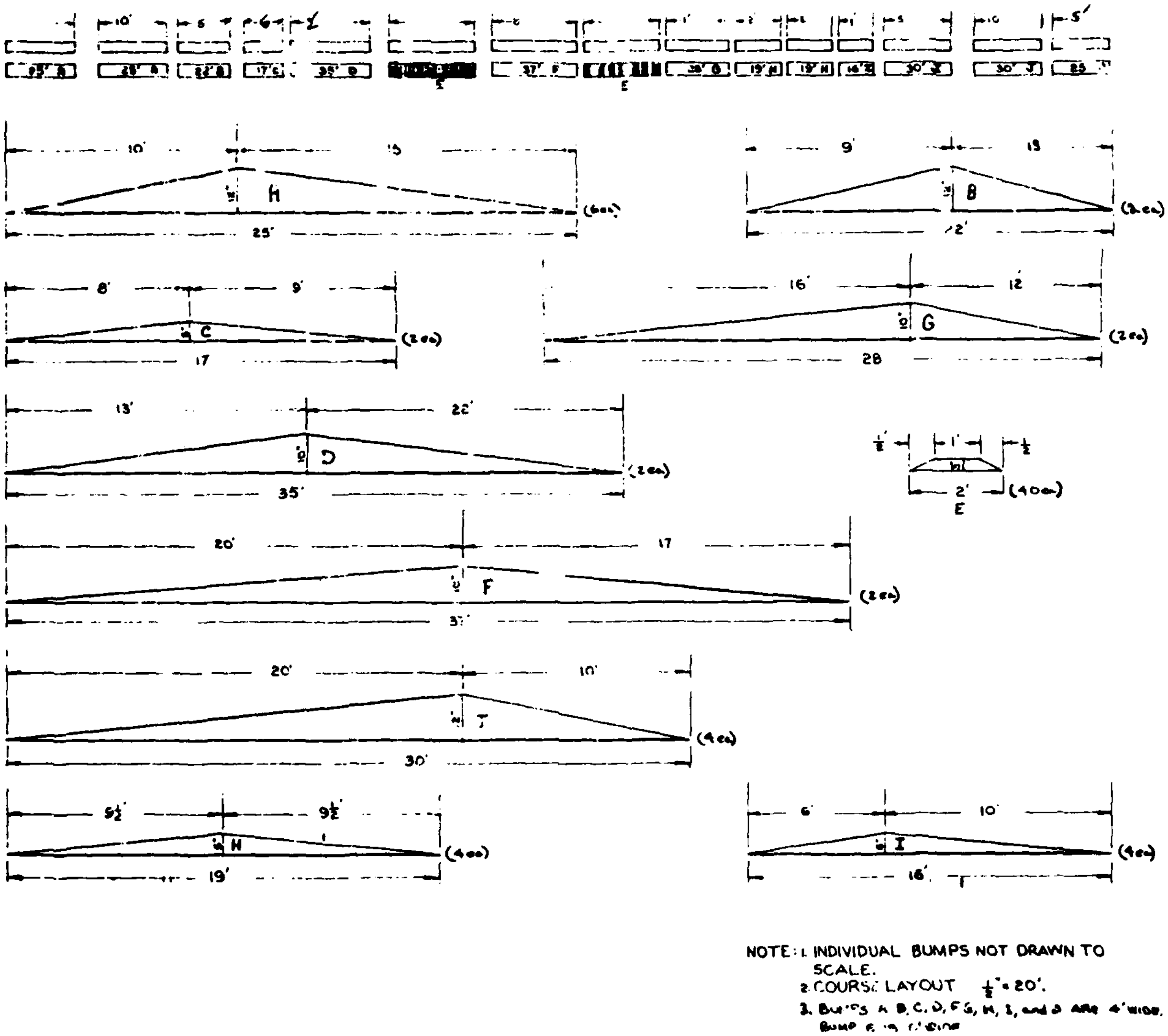

Figure 26. Belgium block ramps.

(a)

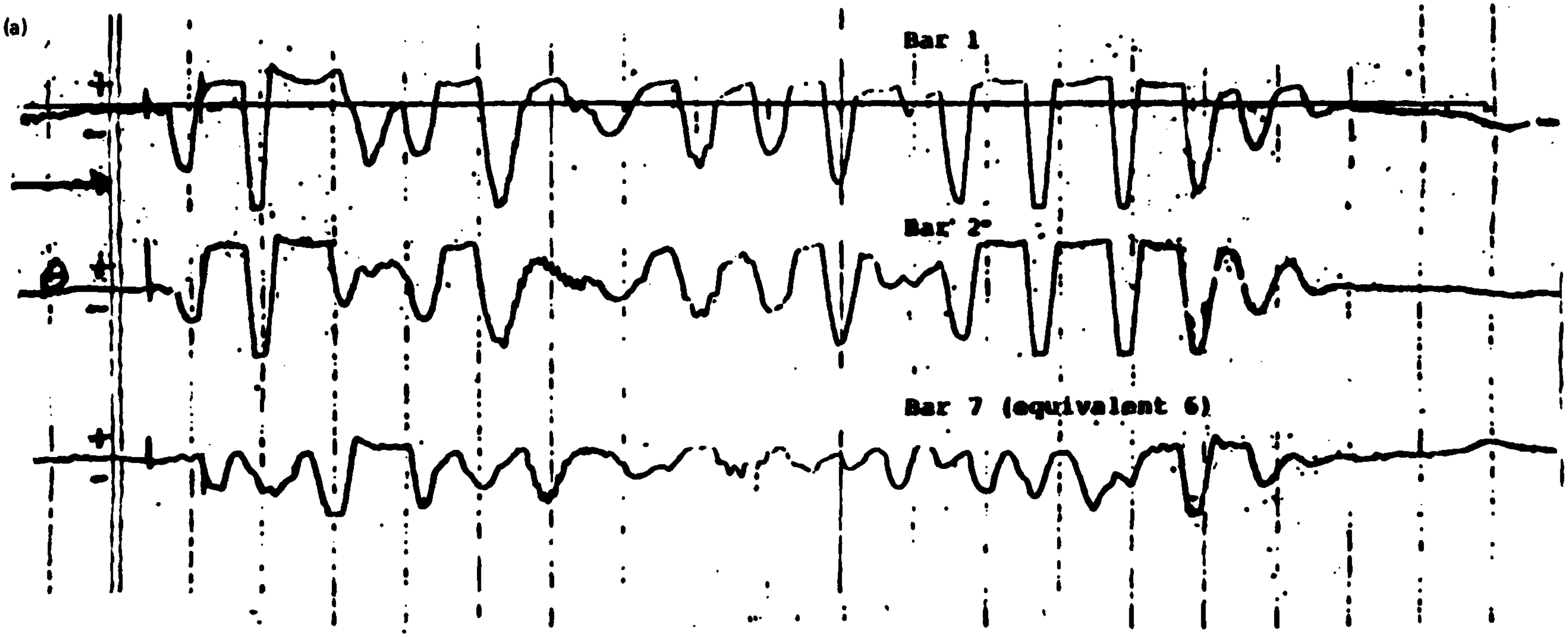

Amplitude Distribution Data
(course length 462 ft)

(b)

	+ Peak	- Peak	+ 99%	- 99%	+ 66%	- 66%	+ 50%	+ 25%	- 25%
BAR 1	15.47	-30.71	15.33	-28.44	8.81	-3.51	3.00	-8.04	10.91
BAR 2	21.70	-28.92	21.42	-26.80	8.41	-7.43	-1.06	-11.53	13.92
BAR 7	13.91	-30.61	13.76	-30.47	6.63	-2.39	2.56	- 7.19	8.35

Figure 27. Load spectrum (run #48 - speed 25 mph).

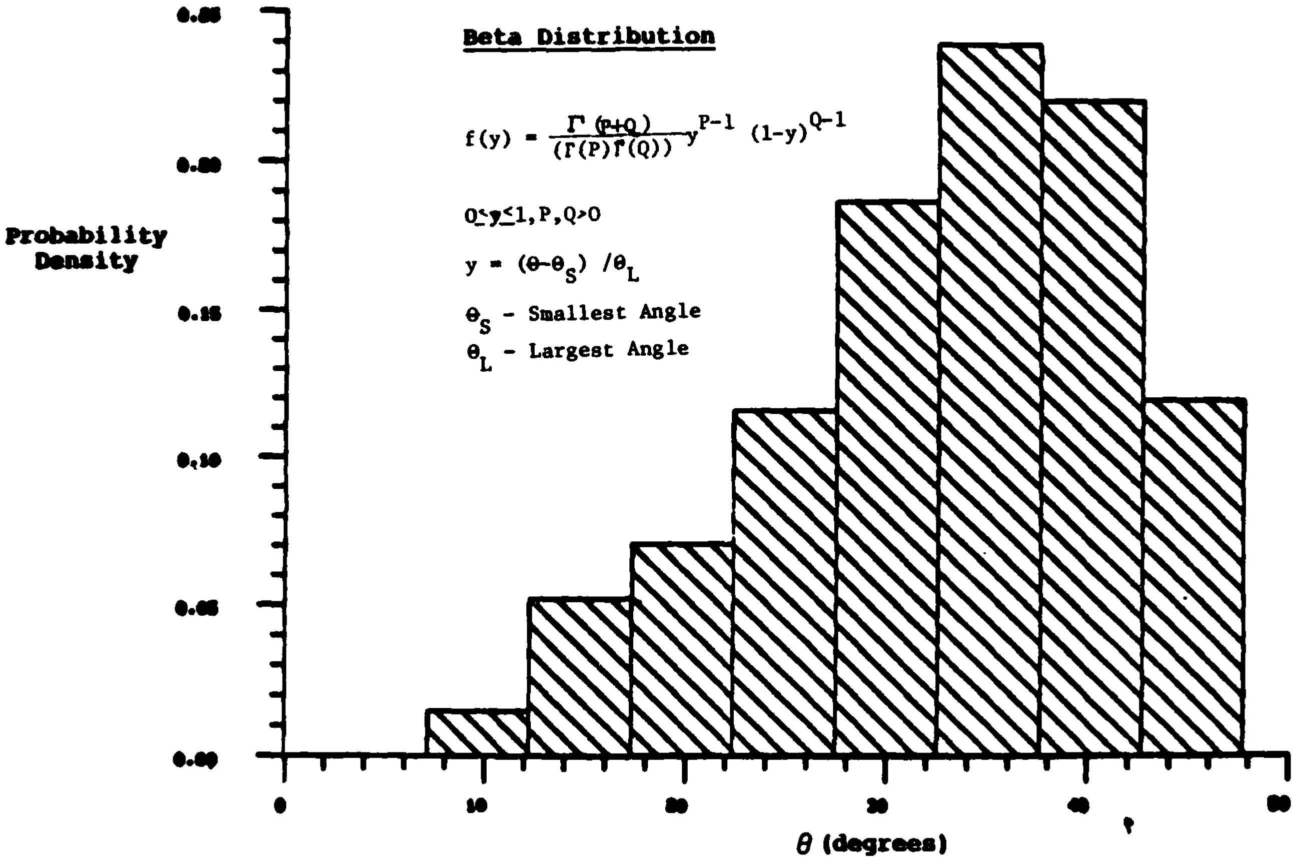

Figure 28. Spectrum load representation (run no. 48 - speed 25 mph).

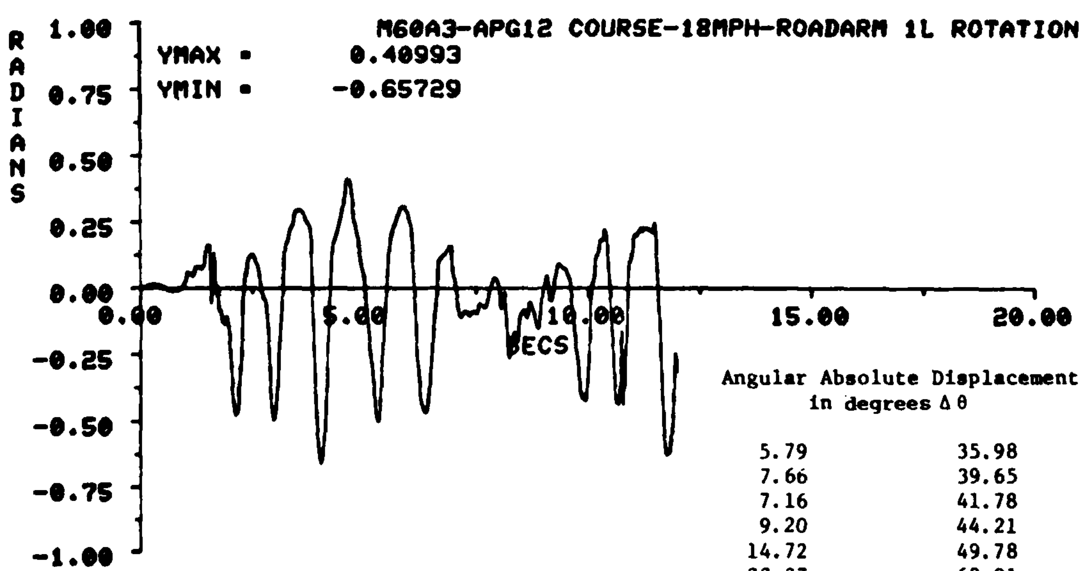

Angular Absolute Displacement in degrees Δθ

5.79	35.98
7.66	39.65
7.16	41.78
9.20	44.21
14.72	49.78
22.37	62.01
30.02	

Figure 29.

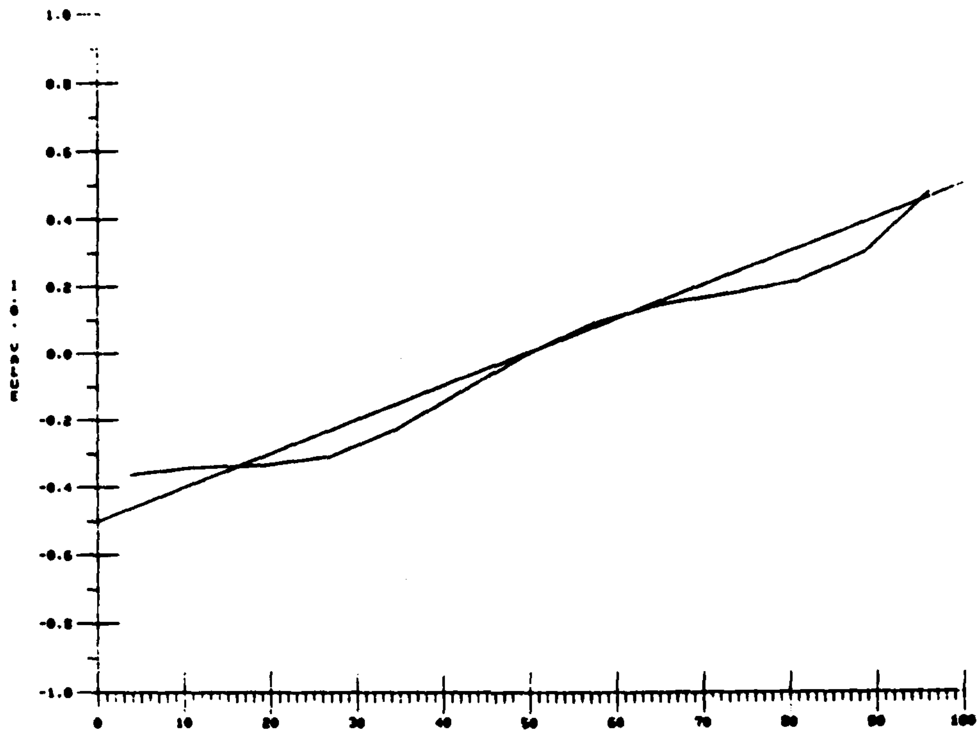

(a)

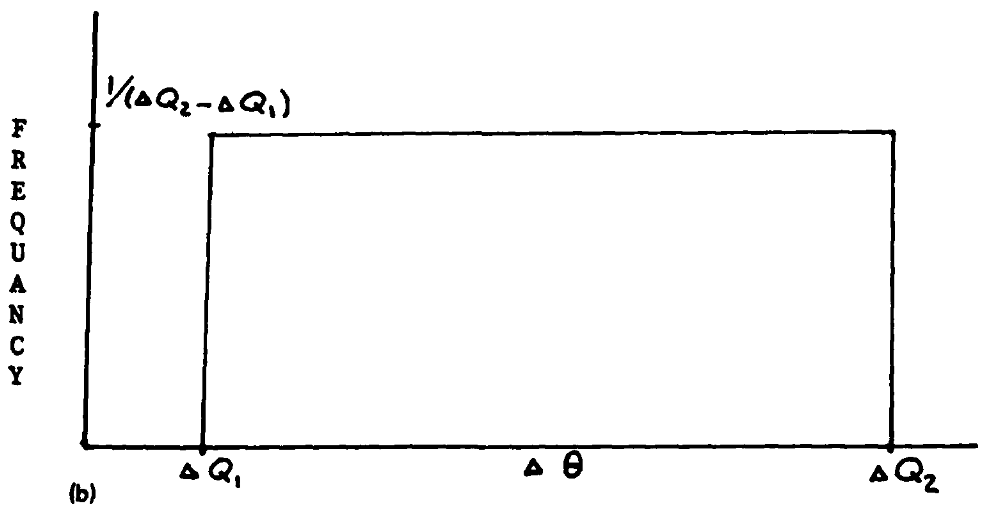

(b)

Figure 30. (a) I.Q. plot (18 mph/1L) , and (b) uniform distribution.

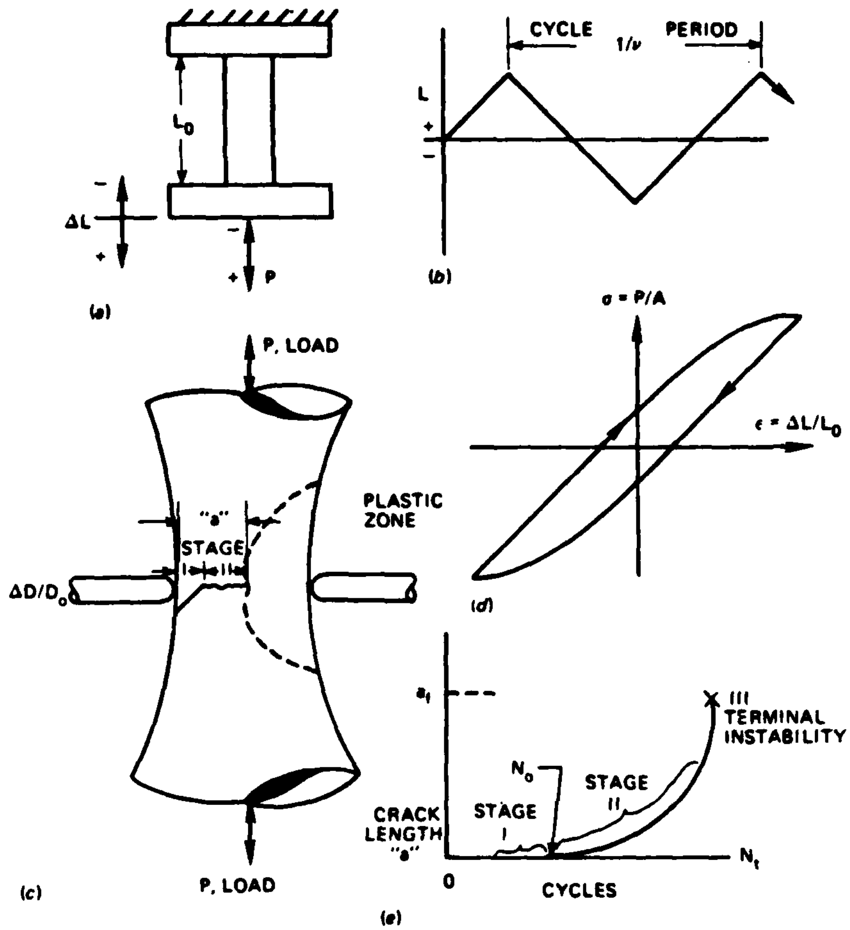

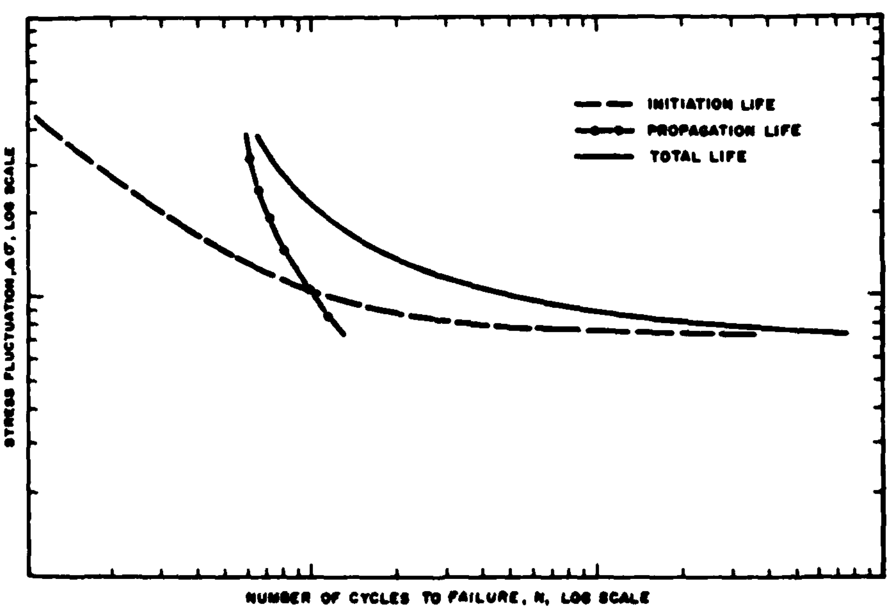

Figure 31. Schematic S-N curve divided into initiation and propagation components.

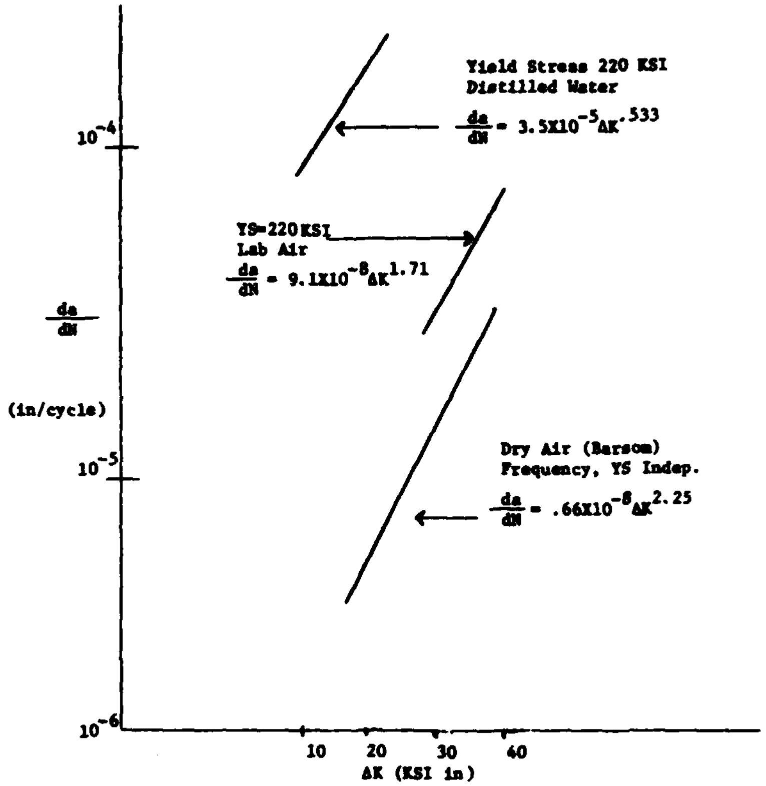

Figure 32. Determination of cycles to failure (LEFM appr.).

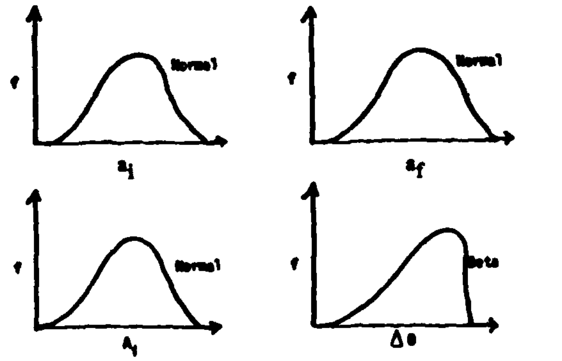

$$\int_{-\infty}^{X} f_i \, dX = R$$

R = UNIFORM RANDOM NUMBERS

f_i = FREQUENCY DISTRIBUTION

$\bar{a}_i$ = .001 in. [C.V. = 5,10,15 Percent]

$\bar{a}_f$ = .0133 in.

$\bar{A}_2$ = 3.29 (Spline Region) Ksi $\sqrt{in}$

Figure 33.

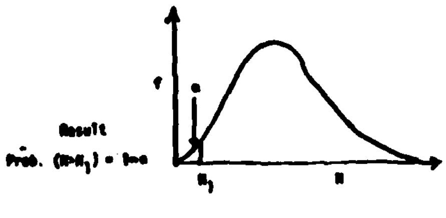

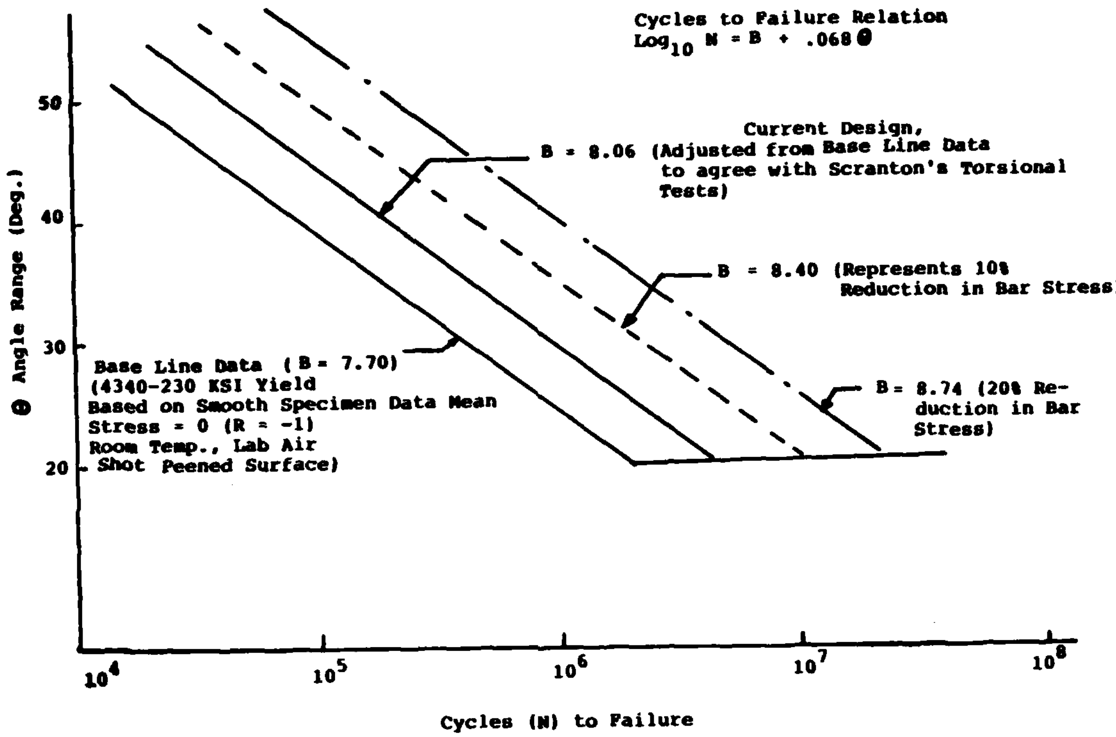

Figure 34. Torsional fatigue life.

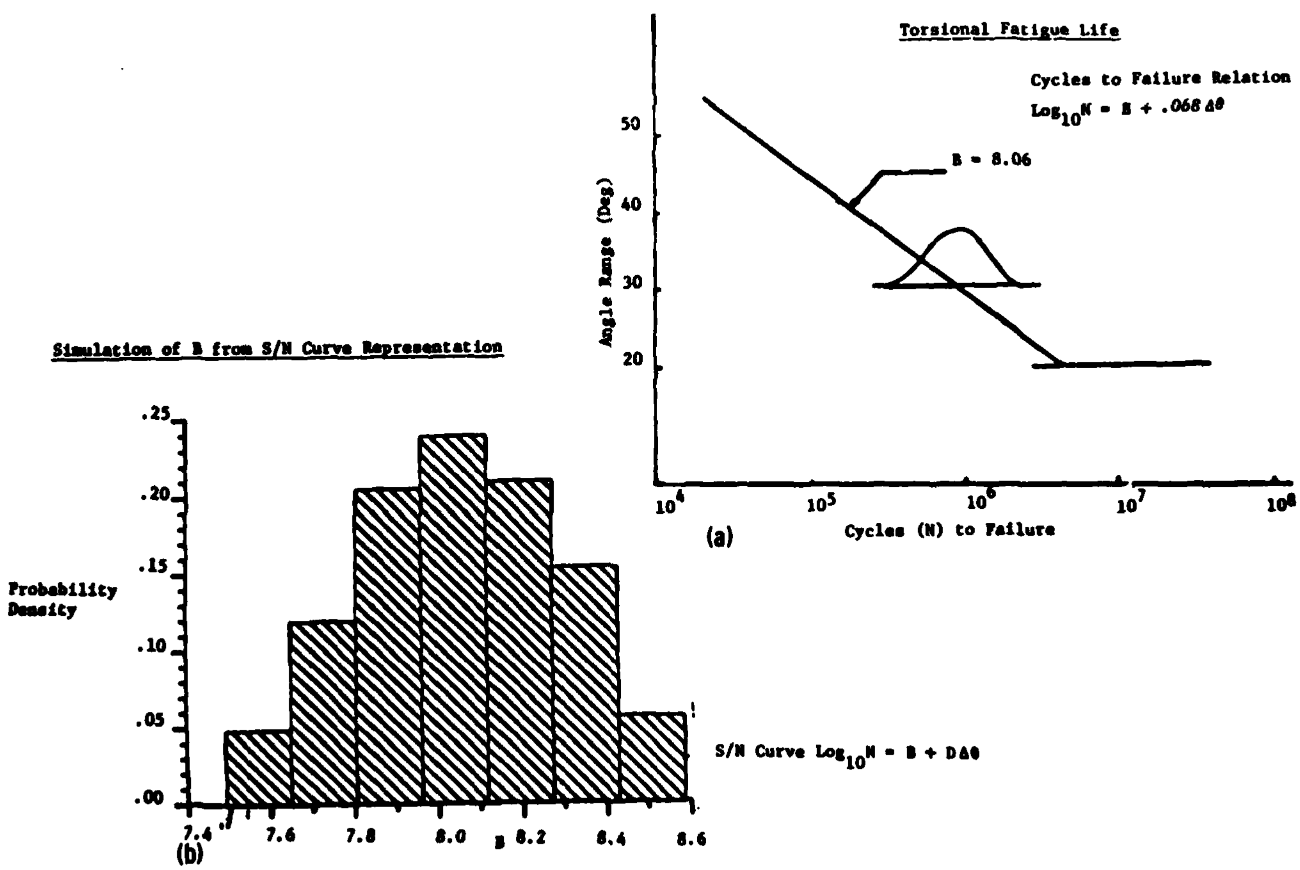

Figure 35.

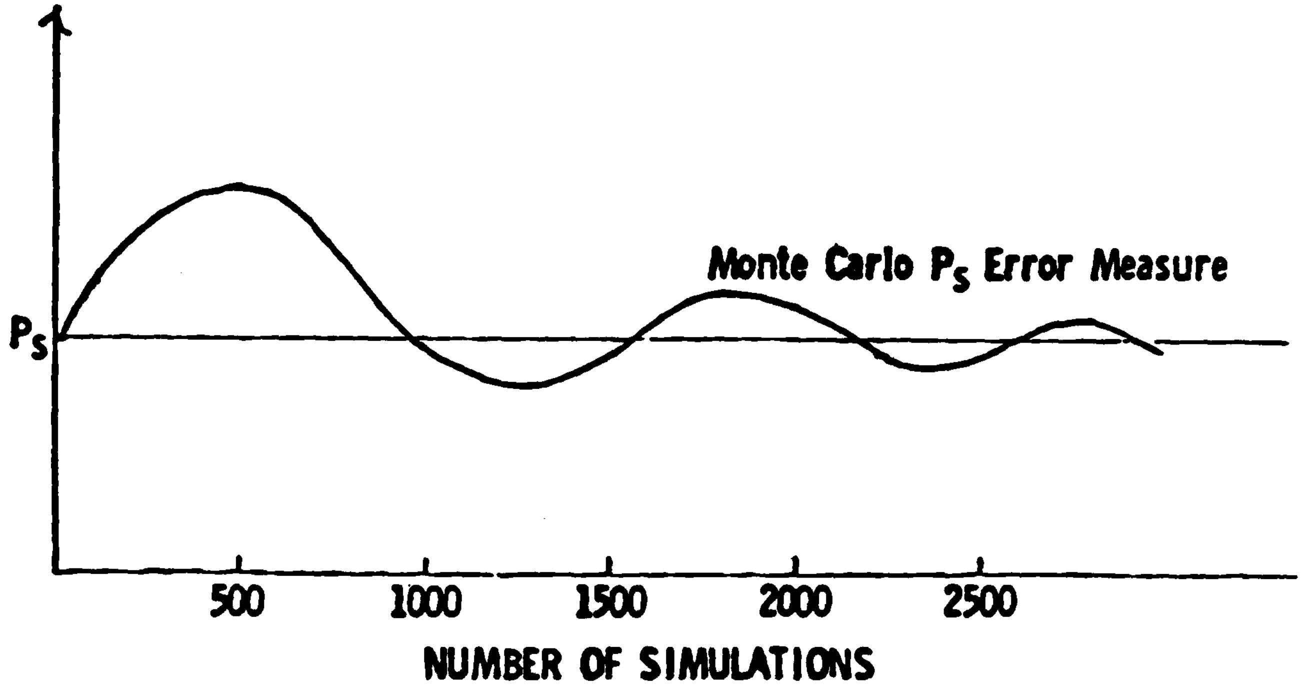

Figure 36. Additional criteria: convergence of 3rd and 4th moments.

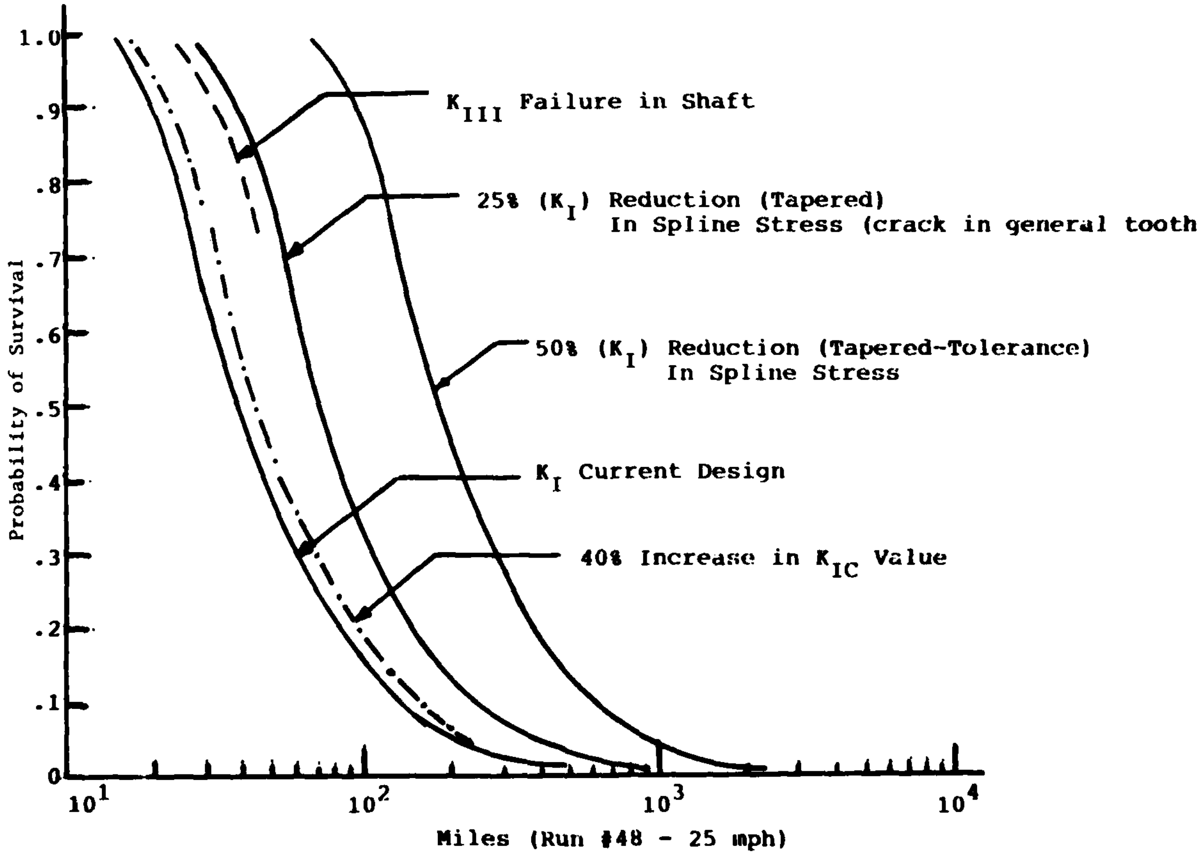

Figure 37. Torsion bar reliability - probability of survival versus miles - da/dN relationship.

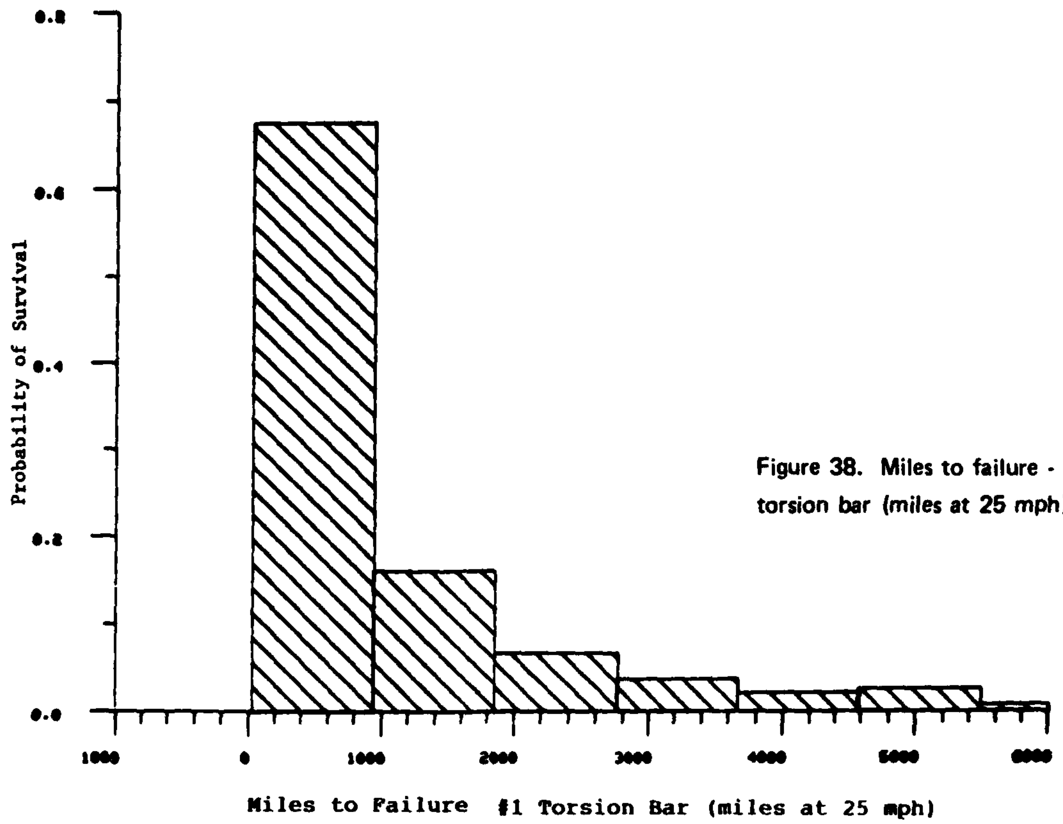

Figure 38. Miles to failure - no. 1 torsion bar (miles at 25 mph).

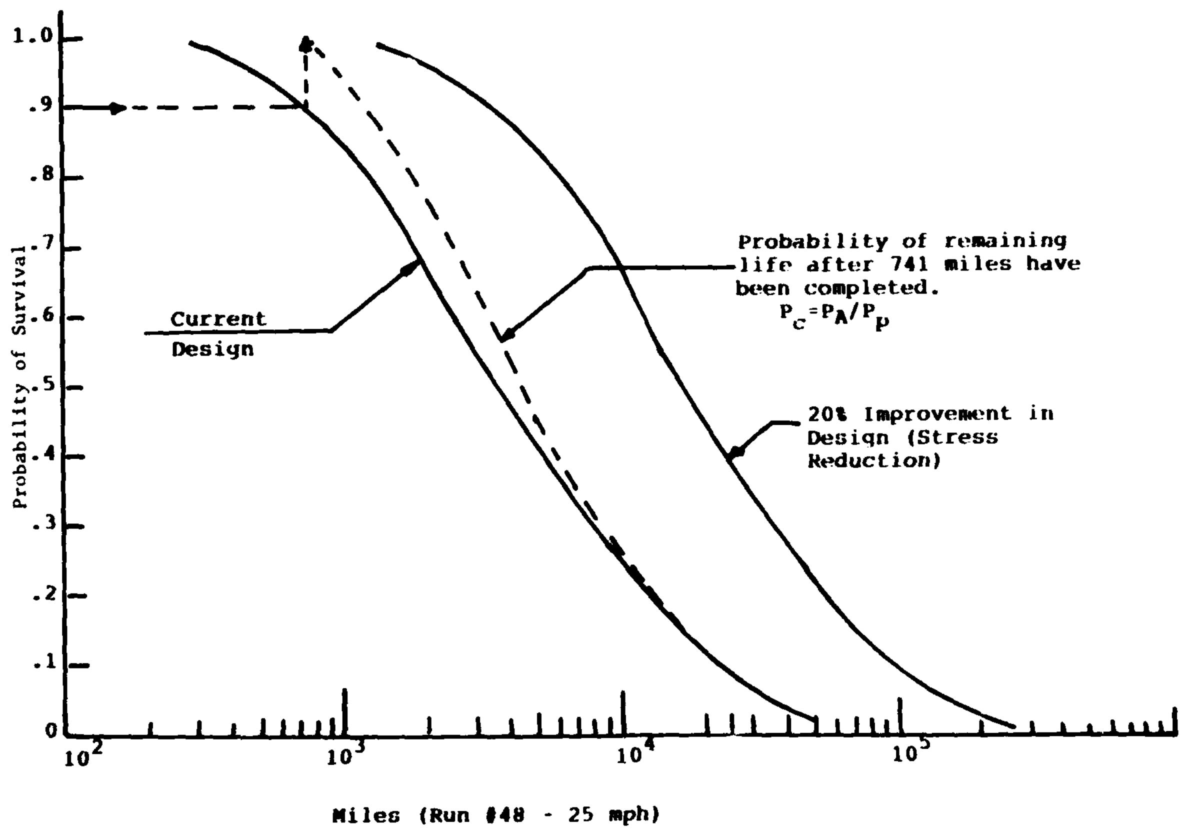

Figure 39. Probability of survival versus miles - S/N curve results.

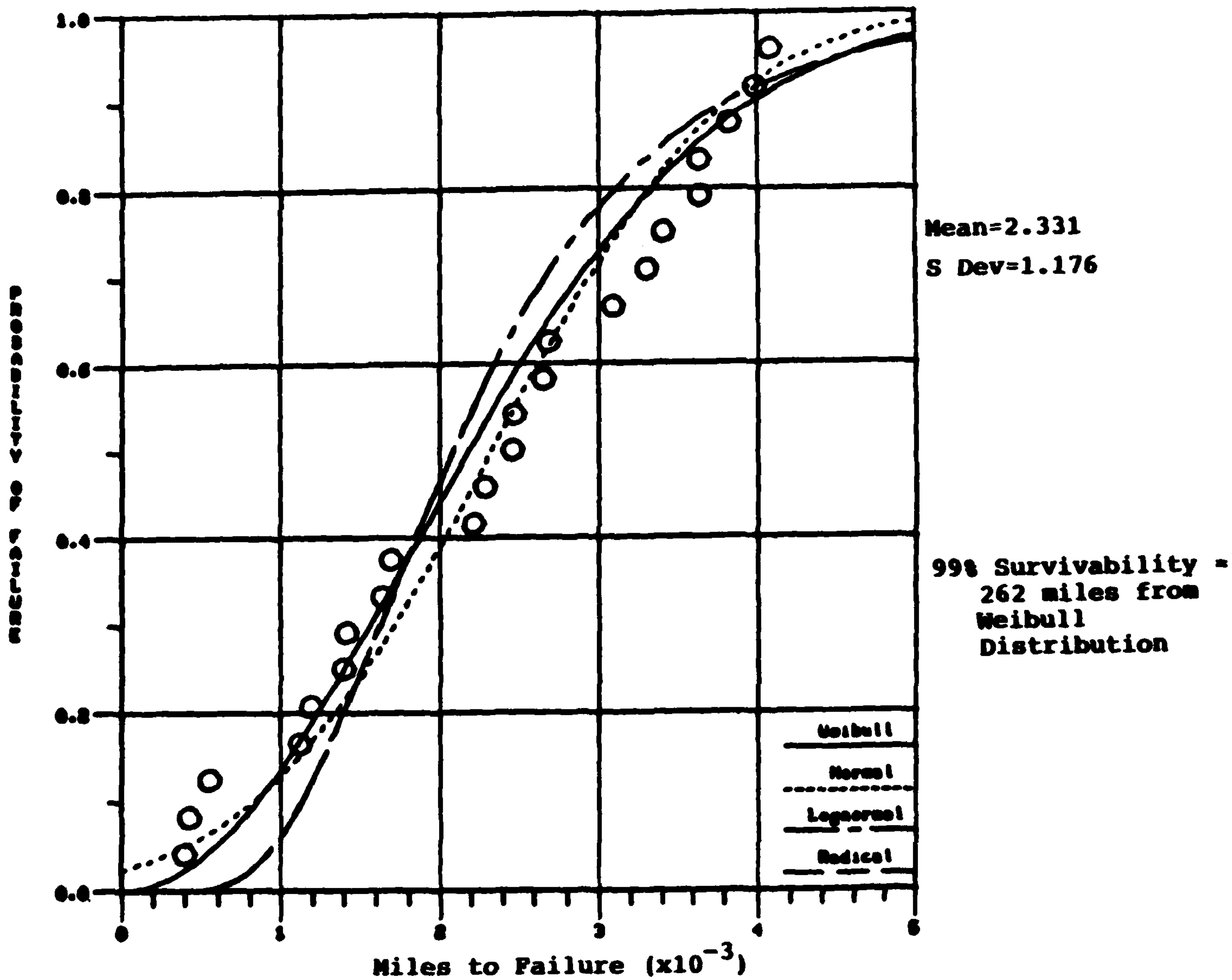

Figure 40. APG reported failure - no. 1 torsion bars - (R and L together).

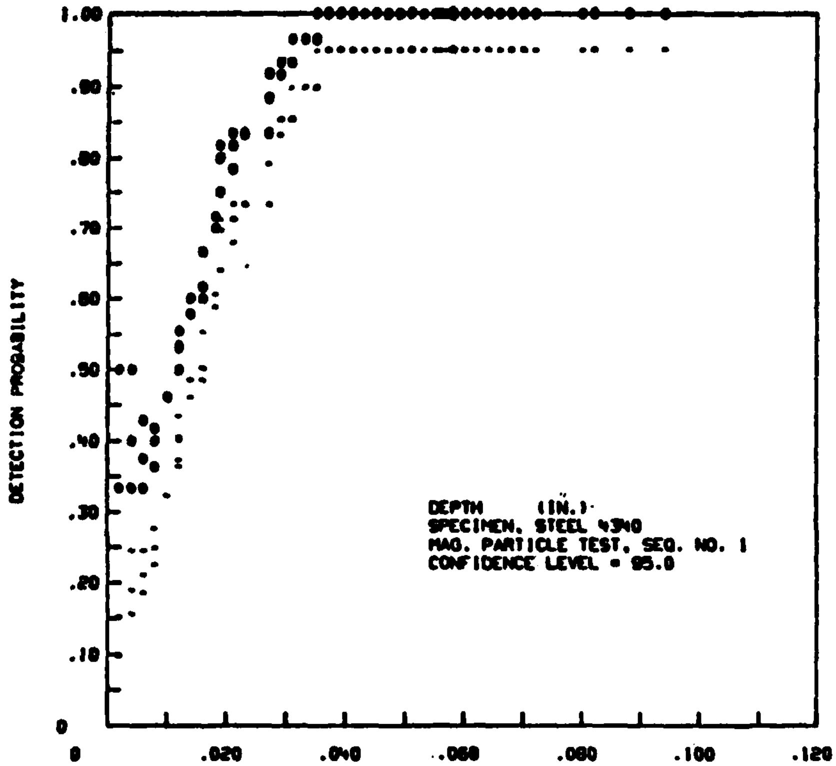

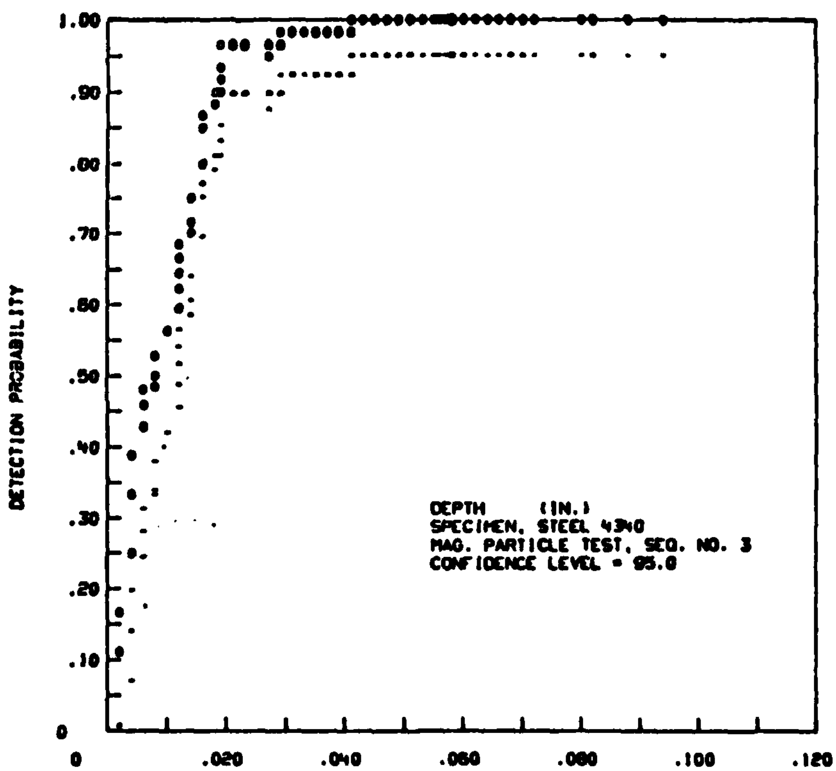

Figure 41. Crack detection probability of the magnetic particle inspection method for steel specimens plotted by actual crack depth at 95% confidence.

Table 1. SCRANTON FATIGUE TEST RESULTS

Date	Heat Code	Total Cycles	Location of Break
77	JAB	45,072	Test stopped - repair machine
77	JAF	245,157	Failure
77	JAK	284,560	Failure
78	JAE R	108,744	Small end radius
78	JBG R	137,917	Test stopped - repair machine
78	JBG R	246,867	Test stopped - repair machine
78	JBI	181,344	24" from large end
78	JBI	310,785	38" from large end
78	JBI	195,863	18" from large end
78	JBD	362,016	18" from large end
78	JBK	270,778	19" from large end
78	JAO	113,341	Failure
78	JAT	248,105	Test stopped - repair machine
78	JBA	105,821	Test stopped - repair machine
78	JBB	273,434	Test stopped - repair machine
78	JBD	357,023	Test stopped - repair machine
78	JBC	207,889	Failure
78	JBG	186,849	Failure
79	JBL	239,396	Small end radius
79	JBI	147,773	Small end radius
79	JBL (2)	271,990	18" from large end
79	JBR	394,758	Machine failure
79	JBS	221,500	Small end radius
79	JBP	137,765	Small end radius
79	JBT	248,754	12" from small end
79	JBL (2)	201,169	Small end radius
79	JBL (2)	331,606	46" from large end
79	JBZ	144,300	Small end radius
79	JBV	125,955	24" from large end
79	JCB	196,560	Small end radius
79	JBL (2)	123,325	Small end radius
79	JBL (2)	219,715	Small end radius
79	JCC	99,439	Small end radius
79	JCD	230,325	6" from large end
79	JBL (2)	190,373	16" from large end
79	JBL (2)	156,315	Small end radius
79	JBL (2)	56,361	Small end radius
79	JBL (2)	142,939	26" from large end
79	JBL (2)	131,890	Small end radius
79	JCF	119,840	Small end radius
79	JCG	281,225	21" from large end
79	JCI	149,815	Small end radius
79	JBX	88,624	Small end radius
79	JBX	67,784	Large end radius
79	JCD	114,986	40" from large end
79	JCD	107,273	42" from large end
79	JCJ	190,044	8" from large end
79	JCK	190,050	Machine failure
79	JCT	192,170	Small end radius
79	JCS	133,677	Test stopped - repair machine
79	JCU	254,788	Small end radius
79	JCP	85,815	Test stopped - repair machine
79	JCO	45,437	Test stopped per L. R. suggestion
79	JCW	48,125	Test stopped per L. R. suggestion
80	JCX	108,158	Small end radius
80	JCO	260,376	Large end radius
80	JCZ	325,230	Machine failure
80	JCW	265,255	Machine failure
80	JCY	128,628	14" from large end
80	JCX	246,789	14" from small end
80	JCW	264,318	14" from large end
80	JHF	84,728	Test stopped - repair machine
80	JHG	77,608	Test stopped - repair machine
80	JHE	151,301	12" from small end
80	JBX	183,740	50" from large end

Table 1. Continued

Date	Heat Code	Total Cycles	Location of Break
80	JHL	140,401	Test stopped per L. R. suggestion
80	JHK	52,492	Test stopped per L. R. suggestion
80	JBX	107,417	62" from large end
80	JHP	222,374	Test stopped per L. R. suggestion
80	JCX	92,028	Test stopped per L. R. suggestion
80	JHP	46,249	Test stopped per L. R. suggestion
80	JHP	135,232	6" from large end
80	JHP	80,517	Large end radius
80	JHP	214,090	48" from large end
80	JKP	167,191	Test stopped per L. R. suggestion
80	JKR	45,092	Test stopped per L. R. suggestion
80	JKS	298,271	60" from large end
80	JKD	123,265	Small end radius
80	JGX	75,850	34" from large end
80	JBY	56,600	32" from large end
81	JLI	136,800	Test stopped per L. R. suggestion
81	JLG	92,700	Test stopped per L. R. suggestion
81	JLE	87,250	Test stopped per L. R. suggestion
81	JLF	231,750	Small end radius
81	JLH	78,440	Test stopped per L. R. suggestion
81	JLW	52,840	Test stopped per L. R. suggestion
81	JLX	125,140	Test stopped per L. R. suggestion
81	JLY	88,500	Test stopped per L. R. suggestion
81	JMD	180,320	Test stopped per L. R. suggestion
81	3MM	115,225	54" from large end
81	JND	269,811	Test stopped per L. R. suggestion
81	JNA	217,368	Machine failure
81	JMP	267,951	Test stopped per L. R. suggestion
81	JNC	88,192	Test stopped per L. R. suggestion
81	JNR	85,715	Test stopped per L. R. suggestion
81	JLT	95,703	Test stopped per L. R. suggestion
81	JLI	80,570	8" from large end
81	JLI	175,235	Test stopped per L. R. suggestion
81	JLI	146,881	Test stopped per L. R. suggestion
81	JLI	127,877	30" from large end
81	JLI	244,732	18" from large end
81	JLI	193,882	Machine failure
81	JLI	227,500	42" from large end
81	JLI	288,725	Test stopped per L. R. suggestion
81	JOM	223,629	Small end radius
81	JOP	443,417	30" from small end
81	JKT	100,607	60" from large end
81	JLT	49,422	60" from large end
81	JKT	75,488	61" from large end
81	JKT	71,488	Small end radius
81	JLT	41,802	70" from large end
81	JLR	-	46" from large end
82	JOR	212,084	Large end radius
82	JPB	350,769	46" from large end
82	JOP	301,591	24" from large end
82	JPB	303,336	Small end radius
82	JPC	584,366	18" from small end
82	JOS	268,040	Machine failure
82	JOS	228,710	20" from large end
82	JPC	358,269	Machine failure
82	JNL	77,990	48" from large end
82	JNL	57,409	44" from large end

Date	Bar No.	New Cycles To Failure	Location of Break
82	1	185,000	Machine broke
82	2	148,000	Machine broke
82	3	544,000	Test stopped
82	4	447,696	Failed
82	5	240,348	Failed (was broken in MI machine)
82	6	362,771	Machine broke
82	7	367,307	Test stopped

All New Spline Design

A failed torsion bar from Ft. Knox spline failure?
M60-A3. Will be sent to Hickey.

Table 2. CHEMICAL COMPOSITION

Source/Marking	Weight Percent GD/JN	MPU #5399	Specification AISI 8660 Minimum	Specification AISI 8660 Maximum
Carbon	0.63	0.54	0.55	0.65
Manganese	0.87	-	0.75	1.00
Phosphorus	0.009	-	-	0.04
Sulfur	0.02	0.02	-	0.04
Silicon	0.21	-	0.20	0.35
Nickel	0.58	-	0.04	0.70
Chromium	1.02	-	0.04	0.60
Molybdenum	0.15	-	0.15	0.25

Table 3. ROCKWELL C HARDNESS

Source/Marking Location	GD/JN Spline Traverse	GD/JN Body Traverse	MPU #5399 Spline
HRC	(48.0 - 50.3)	(48.5 - 49.9)	50.0

Table 4. TENSILE PROPERTIES OF GD/JN TORSION BAR

Orientation	0.2% Y.S. (ksi)	U.T.S. (ksi)	Elon. (%)	R.A. (%)
Long.	231.4	257.2	8.3	28.4
	229.6	258.1	8.7	28.5
	230.5	257.7	8.5	28.5

Table 5. ENERGY AND FIBROSITY DATA FOR GD/JN

Longitudinal Orientation (LR)

Testing Temp. (°C)	Charpy Impact Energy (ft-lb)	Fibrosity (%)
-40 (-40°F)	5.5	5
+22 (+72°F)	7.7	10
+100 (+212°F)	7.9	15
+160 (+320°F)	8.8	50
+180 (+356°F)	11.0	80
+220 (+428°F)	9.0	100
+240 (+464°F)	8.5	100

Transverse Orientation (TR)

Testing Temp. (°C)	Charpy Impact Energy (ft-lb)	Fibrosity (%)
+22 (+72°F)	3.5	5
+22 (+72°F)	1.8	5
	2.7	5
-40 (-40°F)	2.8	5
-40 (-40°F)	3.0	5
	2.9	5

Table 6. FRACTURE TOUGHNESS

Source/Marking	Orientation	K_Q, ksi $\sqrt{in.}$ Testing Temp. (°C) RT	-40
GD/JN	LR	45.7	32.2
		40.3	24.7
		43.0	28.5
	TR	38.9	32.1
		37.7	31.8
		38.3	32.0
MPU #5399	TR	34.5	
		33.9	
		34.2	

Table 7. SPECTRUM LOAD (PROFILE IV COURSE) - BETA FUNCTION REPRESENTATION

Cumulative Probability	Test Results θ^A (Degree)	Beta Representation θ^A (Degree)
	Run 40 (5 mph)	
0.10	0.14	0.86
0.25	4.4	5.8
0.34	5.0	7.2
0.50	8.6	9.3
0.66	12.5	11.5
0.75	14.2	12.7
0.99	17.0	16.7
	Run 42 (10 mph)	
0.10	14.0	6.1
0.25	16.0	19.2
0.34	22.8	21.5
0.50	25.8	24.8
0.66	29.7	27.6
0.75	30.6	29.0
0.99	32.6	32.5
	Run 48 (25 mph)	
0.10	2.3	10.8
0.25	22.7	26.2
0.34	27.2	29.1
0.50	33.7	33.3
0.66	39.5	37.1
0.75	41.6	39.3
0.99	46.0	46.9

Cumulative time probabilities of torsional bar angular displacement θ adjusted to positive range by $\theta^A = \theta + |\theta^-|$ where θ^- = maximum negative angular displacement.

Table 8. MINIMUM LIFE ESTIMATES (99% SURVIVABILITY)
da/dN CURVE RESULTS

Velocity (mph)	Mileage Expected (Function of Spline Stress) Current Design	Mileage Expected (Function of Spline Stress) 25% Reduction	Mileage Expected (Function of Spline Stress) 50% Reduction
5	71.0	138.0	341.0
10	29.9	51.9	143.0
15	15.2	29.3	72.3
20	14.0	26.9	66.3
25	14.2	28.4	70.2

Table 9. MONTE CARLO RESULTS FOR S/N CURVE MINIMUM LIFE ESTIMATE (99% PROBABILITY OF SURVIVAL) VERSUS VELOCITY (MPH)

Velocity (mph)	Mileage Expected (Current Design)	Mileage Expected (10% Design Improvement)	Mileage Expected (20% Design Improvement)
5	6974	9474	12970
10	2000	3138	4420
15	345	633	1089
20	276	515	860
25	292	557	865

Note: A 99% survivability estimate of 262 miles was obtained from cumulative APG mileage on vehicles at time of torsion bar failure. Velocity of vehicle during tests was approximately 15 to 25 mph.

Table 10. TORSION BAR SPRING FAILURES FROM SELECTED APG TESTS, SEPTEMBER 1979-April 1982*

Vehicle Type	TECOM Project Number	APG Report Number	Number Failed	Vehicle Position,† Number and Side	Cumulative APG Mileage on Vehicle at Time of Failure
M60A1E3	1-VC-080-060-083;PV-1	APG-MT-5376	9	1R,1L,6L,2R,4R, 5R,1R,1L,1R	1643, 1693, 1860, 2387, 2387, 2387, 2463, 2471, 2686
"	" ;PV-2	"	3	1L,1L,6R	2286, 3086, 3640
"	" ;PV-3	"	2	4L,4R	3025, 3025
"	" ;PV-4	"	3	1L,1R,4L	1127, 2218, 3093
"	" ;PV-5	"	5	1R,6L,5L,1L,6R	1190, 1988, 3306, 4085, 4171
"	" ;PV-6	"	6	1R,5L,5L,1R,1L,1L	546, 2217, 2711, 3303, 3834, 3998
"	" ;PV-7	"	4	1R,1R,1L,6R	3411, 3641, 3641, 3641
M60A1‡	1-VC-080-060-087	APG-MT-5299	2	1R,6R	396, 1596
M60A3	1-VC-08F-060-033	APG-MT-5299	2	1L,6L	1402 average
M60A3**	1-VC-087-060-035	APG-MT-	2	1L,1L	421, 1418
M48A5**‡	3-WE-100-DIV-008	APG-MT-	3	6L,3R,1R	1516, 2638, 2659

*Taken from Appendix II.[12]
†Positions 1, 2, and 6 have shocks attached to the roadwheels.
‡Detailed failure report.[5]
**Discussed in greater detail in this report.

Table 11. PROBABILITY OF SURVIVAL VERSUS MILES - TACOM SIMULATION COURSE

	Probability of Survival (%)	5 mph (38 Displ) 1L	5 mph (38 Displ) 2L	5 mph (38 Displ) 6L	5 mph (12 displ) 1L	18 mph 1L	18 mph 2L	18 mph 6L	25 mph 1L	25 mph 2L	25 mph 6L
Original Design	99	1467			2702	14	16	1324	620	1060	2289
	95	4859			5032	37	45	3107	1478	2594	5441
	90	12550			7433	70	89	5032	2471	4157	8777
	80	13900			11210	176	238	9502	4701	7827	17160
	70					398	590	18350	8354	13930	29280
10% Design Improvement	99	1618			3742	32	37	1941	1010	1660	3363
	95	3527			7694	85	101	4617	2424	3951	7981
	90	5487			11390	159	191	7290	3935	6245	12580
	80	9693			18760	359	467	13680	7246	11570	24010
	70				27860	792	1082	21980	12490	20130	29280
20% Design Improvement	99	2222			5107	65	74	2757	1523	2336	4686
	95	4732			10350	166	193	6321	3618	5623	10590
	90	7359			15420	301	361	9990	5717	8831	16910
	80	12910			25160	652	818	18420	10320	16020	29280

APPENDIX A. TORSIONAL STRESSES IN A NONUNIFORM BAR

Due to the enlargement of the torsion bars at their ends there could be high stress concentrations in the filets caused by the applied torsional moments.

Thermal analogy is used in the analysis of torsional stresses of the nonuniform bars. According to the Michell torsion problem,[1] the angle of twist satisfies the equation

$$\frac{\partial}{\partial r}\left(Gr^3 \frac{\partial \Psi}{\partial r}\right) + \frac{\partial}{\partial z}\left(Gr^3 \frac{\partial \Psi}{\partial z}\right) = 0 \tag{A-1}$$

and the shear stresses are given by

$$\tau_{r\theta} = Gr \frac{\partial \Psi}{\partial r}, \; \tau_{z\theta} = Gr \frac{\partial \Psi}{\partial z} \tag{A-2}$$

where G is the shear modulus, r is the radius from the central axis and Z is the distance along the axis. Using thermal analogy of axisymmetric heat condition and setting,

$$\begin{aligned} &y = r, \; z = z, \; T = \Psi, \; K_y = K_z = Gr^2 \\ &q_B = r\tau_s \end{aligned} \tag{A-3}$$

where T is the temperature, K_y and K_z the conductivity coefficients in the Y and Z directions, and q the heat flux, the problem can be easily solved. By substituting the above quantities in Equation A-1, results in the familiar heat conduction equation of the axisymmetric body

$$\frac{\partial}{\partial y}\left(yK_y \frac{\partial T}{\partial y}\right) + \frac{\partial}{\partial z}\left(yK_z \frac{\partial T}{\partial z}\right) = -yq_B. \tag{A-4}$$

It is to be noted that we could have used the substitution $K_y = K_z = Gr^3$, resulting in the plane heat conduction problem. However, the error in the analysis would be much greater due to the combining of the term Gr^3 rather than Gr^2 in every element. The analysis would then be carried out using the standard heat conduction finite element codes.

1. TIMOSHENKO, S. and GOODIER, J. N. *Theory of Elasticity*. McGraw-Hill, New York, 1951.

APPENDIX B. ST. VENANT TORSIONAL STRESSES OF MULTIPLY CONNECTED REGIONS

The existence of subsurface cracks in the torsion bar due to inclusions and poor material is a possibility. The evaluation of stress intensity factors for these cracks requires the solution of a St. Venant torsion problem of a multiply connected region which is:

$$\frac{\partial^2\phi}{\partial x^2} + \frac{\partial^2\phi}{\partial y^2} = -2G\theta. \tag{B-1}$$

The stresses are determined from

$$\tau_{xz} = \frac{\partial\phi}{\partial y},\ \tau_{yz} = -\frac{\partial\phi}{\partial x} \tag{B-2}$$

with G the shear modulus and θ the angle of rotation. The boundary conditions are

$$\frac{\partial\phi}{\partial s} = 0 \tag{B-3}$$

on the outer boundary and

$$\oint_{\Gamma_i} \partial\phi/\partial n \quad ds = 2G\theta A_i \tag{B-4}$$

where A_i are the areas of the interior holes or crack regions and Γ_i is the boundary. For the case of a shaft with one or two subsurface cracks or holes, ϕ can be chosen to be zero on the outer boundary and hence satisfy the boundary condition Equation B-3. While for other interior boundaries Γ_i, Equation B-4 can be substituted equivalently with $\phi = A_i$. The constants A_i will remain undetermined and can be found from the solution of Equation B-1 together with the equilibrium equations for the whole section.

The other alternative is to use the condition $\partial\phi/\partial s = 0$ on all boundaries, which also complicates the solution of the differential Equation B-1.

The approach used here is based on the penalty function method.[1] In the equation, B-1 is cast in a variational problem where

$$I = \int_v \left[(\frac{\partial\phi}{\partial x})^2 + (\frac{\partial\phi}{\partial y})^2 - 2G\theta\phi\right] dv = \text{min}. \tag{B-5}$$

subject to the condition $\partial\phi/\partial s = 0$ on all free boundaries.

1. REDDY, J. N. *Penalty - Finite Element Methods in Mechanics.* ASME, AMD, v. 51, 1982.

Using the penalty function method, Equation B-5 is written in the following form:

$$I_p = \int_v \left[\left(\frac{\partial\phi}{\partial x}\right)^2 + \left(\frac{\partial\phi}{\partial y}\right)^2 - 2G\theta\phi \right] dv + \frac{1}{2}\gamma_p \int_{\Gamma_i} \left(\frac{\partial\phi}{\partial s}\right)^2 ds \qquad \text{(B-6)}$$

where γ_p is the penalty parameter and is taken as a very large number thus guaranteeing $\partial\phi/\partial s$ to be very small and close to zero.

The minimization of Equation B-6 gives the heat equations of a two-dimensional problem with the same analogy as in Appendix A. The penalty members are linear heat condition elements (beam like) with very large (or infinite) conductivity.

DISTRIBUTION LIST

No. of Copies	To
2	Commander, Defense Technical Information Center, Cameron Station, Building 5, 5010 Duke Street, Alexandria, VA 20301
1	Commander, U.S. Army Materiel Command (AMC), 5001 Eisenhower Avenue, Alexandria, VA 22333
	Commander, U.S. Army Tank-Automotive Command, Warren, MI 48090
1	ATTN: AMSTA-NS, Dr. H. Dobbs
1	AMSTA-RC, Mr. M. Keifesh
1	AMCPM-M60, COL J. A. Logan
1	AMCPM-M60, Mr. R. DeGroot
1	AMCPM-M1, Mr. A. Jokubaitis
1	AMCPM-GCM-L, Mr. J. Chapin
1	AMCPM-FVS, BG C. B. Donovan
1	AMCPM-FVS-Q, Mr. R. A. Gasparski
1	AMCPM-M9, LTC R. F. Huttner
1	AMCPM-LA, COL B. L. McClain
1	AMSTA-H, Mr. R. L. Swint
1	AMSTA-QK, Mr. W. McGinley
1	AMSTA-T, Mr. G. Newcomb
1	AMSTA-Z, COL W. Chandler
1	Tech. Management Dis., Mr. M. McCoulough
	Commander, Aberdeen Proving Ground, MD 21005
1	ATTN: STEAP-MT-G, Mr. J. A. Robinson, Material Testing Directorate
1	STEAP-MT-G, Mr. R. A. McKinnon
1	STEAP-MT-D, Mr. A. Cummings
	FMC Corporation, Ordnance Engineering Division, 1105 Colman Avenue, San Jose, CA 95108
1	ATTN: Mr. A. J. Austin
1	Mr. R. Hare
1	Mr. G. L. Boerman
	FMC Corporation, Steel Products Division, 2101 West 10th Street, Box 1030, Anniston, AL 36201
1	ATTN: Mr. J. P. Lewis
	General Dynamics, Fort Worth Division, P.O. Box 748, Fort Worth, TX 76101
1	ATTN: Mr. L. M. Smith
	Jet Propulsion Laboratory, 4800 Oak Grove Drive, Pasadena, CA 91109
1	ATTN: Dr. D. M. Anderson
1	Dr. Levy Reinhart
	Bolt-Beranek & Newman, Inc., 10 Moulton Street, Cambridge, MA 02138
1	ATTN: Mr. A. Galaitsis
	General Dynamics, Land Systems Division, P.O. Box 1852, Warren, MI 48090
1	ATTN: Mr. E. Hirych

No. of Copies	To
	Commander, U.S. Army Engineer Waterways Experiment Station, Vicksburgh, MS 39180
1	ATTN: Mr. C. Nuttall
1	Mr. N. Murphy
	Battelle Columbus Laboratories, 505 King Avenue, Columbus, OH 43201
1	ATTN: Library
	Director, Army Materials and Mechanics Research Center, Watertown, MA 02172-0001
2	ATTN: AMXMR-PL
7	Authors

☆ U.S. GOVERNMENT PRINTING OFFICE: 1985--502-244--20112

Army Materials and Mechanics Research Center
Watertown, Massachusetts 02172-0001
RELIABILITY AND LIFE PREDICTION METHODOLOGY - M60 TORSION BARS -
Roshdy S. Barsoum, Wayne M. Bethony, Robert H. Brockelman, Harold P. Hatch, Charles F. Hickey, Jr., W. T. Matthews, and D. M. Neal

AD________________

UNCLASSIFIED
UNLIMITED DISTRIBUTION

Key Words

Reliability
Life expectancy
Failure

Technical Report AMMRC TR 85-18, June 1985, 57 pp - illus-tables, D/A Project 1L161102AH42,

The life prediction and reliability assessment of the M60 tank torsion bars were obtained from a methodology developed by using several disciplines of engineering and material science. The disciplines are: structural mechanics, fracture mechanics, statistical reliability, mechanical testing, nondestructive examination (NDE), quality assurance (QA), and metallurgical and fractographic evaluations. The methodology was applied in order to assess the means for increasing torsion bar life and enhance the reliability of the M60 tank. Usually, U.S. Army reliability performance is measured in mean miles between failures (MMBF). In order to introduce a more meaningful measure of component acceptability, this report describes the means for obtaining minimum life estimate at a specified probability of survival using the Monte Carlo method. This includes predicting remaining life with known risk and an approach to perform trade-off costs or redesign for increased life. The result is a more meaningful measure of component acceptability. The reliability versus bar life computation indicated a negligible amount of life after a bar flaw was initiated. The minimum life estimates for crack initiation were in good agreement with actual failure results at Aberdeen Proving Grounds.

Army Materials and Mechanics Research Center
Watertown, Massachusetts 02172-0001
RELIABILITY AND LIFE PREDICTION METHODOLOGY - M60 TORSION BARS -
Roshdy S. Barsoum, Wayne M. Bethony, Robert H. Brockelman, Harold P. Hatch, Charles F. Hickey, Jr., W. T. Matthews, and D. M. Neal

AD________________

UNCLASSIFIED
UNLIMITED DISTRIBUTION

Key Words

Reliability
Life expectancy
Failure

Technical Report AMMRC TR 85-18, June 1985, 57 pp - illus-tables, D/A Project 1L161102AH42,

The life prediction and reliability assessment of the M60 tank torsion bars were obtained from a methodology developed by using several disciplines of engineering and material science. The disciplines are: structural mechanics, fracture mechanics, statistical reliability, mechanical testing, nondestructive examination (NDE), quality assurance (QA), and metallurgical and fractographic evaluations. The methodology was applied in order to assess the means for increasing torsion bar life and enhance the reliability of the M60 tank. Usually, U.S. Army reliability performance is measured in mean miles between failures (MMBF). In order to introduce a more meaningful measure of component acceptability, this report describes the means for obtaining minimum life estimate at a specified probability of survival using the Monte Carlo method. This includes predicting remaining life with known risk and an approach to perform trade-off costs or redesign for increased life. The result is a more meaningful measure of component acceptability. The reliability versus bar life computation indicated a negligible amount of life after a bar flaw was initiated. The minimum life estimates for crack initiation were in good agreement with actual failure results at Aberdeen Proving Grounds.

Army Materials and Mechanics Research Center
Watertown, Massachusetts 02172-0001
RELIABILITY AND LIFE PREDICTION METHODOLOGY - M60 TORSION BARS -
Roshdy S. Barsoum, Wayne M. Bethony, Robert H. Brockelman, Harold P. Hatch, Charles F. Hickey, Jr., W. T. Matthews, and D. M. Neal

AD________________

UNCLASSIFIED
UNLIMITED DISTRIBUTION

Key Words

Reliability
Life expectancy
Failure

Technical Report AMMRC TR 85-18, June 1985, 57 pp - illus-tables, D/A Project 1L161102AH42,

The life prediction and reliability assessment of the M60 tank torsion bars were obtained from a methodology developed by using several disciplines of engineering and material science. The disciplines are: structural mechanics, fracture mechanics, statistical reliability, mechanical testing, nondestructive examination (NDE), quality assurance (QA), and metallurgical and fractographic evaluations. The methodology was applied in order to assess the means for increasing torsion bar life and enhance the reliability of the M60 tank. Usually, U.S. Army reliability performance is measured in mean miles between failures (MMBF). In order to introduce a more meaningful measure of component acceptability, this report describes the means for obtaining minimum life estimate at a specified probability of survival using the Monte Carlo method. This includes predicting remaining life with known risk and an approach to perform trade-off costs or redesign for increased life. The result is a more meaningful measure of component acceptability. The reliability versus bar life computation indicated a negligible amount of life after a bar flaw was initiated. The minimum life estimates for crack initiation were in good agreement with actual failure results at Aberdeen Proving Grounds.

Army Materials and Mechanics Research Center
Watertown, Massachusetts 02172-0001
RELIABILITY AND LIFE PREDICTION METHODOLOGY - M60 TORSION BARS -
Roshdy S. Barsoum, Wayne M. Bethony, Robert H. Brockelman, Harold P. Hatch, Charles F. Hickey, Jr., W. T. Matthews, and D. M. Neal

AD________________

UNCLASSIFIED
UNLIMITED DISTRIBUTION

Key Words

Reliability
Life expectancy
Failure

Technical Report AMMRC TR 85-18, June 1985, 57 pp - illus-tables, D/A Project 1L161102AH42,

The life prediction and reliability assessment of the M60 tank torsion bars were obtained from a methodology developed by using several disciplines of engineering and material science. The disciplines are: structural mechanics, fracture mechanics, statistical reliability, mechanical testing, nondestructive examination (NDE), quality assurance (QA), and metallurgical and fractographic evaluations. The methodology was applied in order to assess the means for increasing torsion bar life and enhance the reliability of the M60 tank. Usually, U.S. Army reliability performance is measured in mean miles between failures (MMBF). In order to introduce a more meaningful measure of component acceptability, this report describes the means for obtaining minimum life estimate at a specified probability of survival using the Monte Carlo method. This includes predicting remaining life with known risk and an approach to perform trade-off costs or redesign for increased life. The result is a more meaningful measure of component acceptability. The reliability versus bar life computation indicated a negligible amount of life after a bar flaw was initiated. The minimum life estimates for crack initiation were in good agreement with actual failure results at Aberdeen Proving Grounds.